STUDIES ON THE EFFECT OF ALUMINA AGGREGATES ON THE PERFORMANCES OF ALUMINA-CARBON REFRACTORIES

A

THESIS SUBMITTED IN PARTIAL FULFILLMENT OF THE REQUIREMENT FOR THE DEGREE OF MASTER OF TECHNOLOGY

In

Ceramic Engineering

By

RASHMI RANJAN ROUT

DEPARTMENT OF CERAMIC ENGINEERING

NATIONAL INSTITUTE OF TECHNOLOGY

ROURKELA-769008

STUDIES ON THE EFFECT OF ALUMINA AGGREGATES ON THE PERFORMANCES OF ALUMINA-CARBON REFRACTORIES

A

THESIS SUBMITTED IN PARTIAL FULFILLMENT

OF THE REQUIREMENT FOR THE DEGREE OF

MASTER OF TECHNOLOGY

In

Ceramic Engineering

By

RASHMI RANJAN ROUT

Under the Guidance of

Prof. SWADESH KUMAR PRATIHAR

Mr. BIRENDRA PRASAD

DEPARTMENT OF CERAMIC ENGINEERING

NATIONAL INSTITUTE OF TECHNOLOGY

ROURKELA-769008

CERTIFICATE

*This is to certify that the thesis on "**Studies on the Effect of Alumina aggregates on the performances of Al_2O_3-C refractories**" submitted by Mr.Rashmi Ranjan Rout to the National Institute of Technology, Rourkela in partial fulfillment of the requirements for the award of the degree of Master of Technology in Ceramic Engineering is a record of bonafide research work carried out by him under my supervision and guidance. His thesis, in our opinion, is worthy of consideration for the award of degree of Master of Technology in accordance with the regulations of the institute.*

The results embodied in this thesis have not been submitted to any other university or institute for the award of a Degree.

Mr. B. Prasad
(AGM/Technology/CNC)
OCL INDIA LTD, Rajgangpur

Prof. S.K.Pratihar
Department of Ceramic Engineering
NIT,Rourkela

ACKNOWLEDGMENT

In the first place, I would like to express my heartfelt thanks and deep sense of gratitude to my reverent teacher and honorable research supervisor **Prof. S. K. Pratihar**, for introducing me to the field of the refractory, for his constant encouragement, efficient planning, and valuable guidance during the entire course of my project work.

I gratefully acknowledge **Prof. S. Bhattacharyya**, Head of Department, Ceramic Engineering, NIT,Rourkela for giving me an opportunity to do the project work at OCL INDIA LTD. Rajgangpur and time to time his suggestion for the improvement of the project.

I would like to acknowledge **Mr. A. Sen and Mr. B. Prasad** for their advice, supervision, and crucial contribution, which made them a backbone of this research project and so to this thesis. Their involvement with their originality have triggered and nourished my intellectual maturity that I will benefit from, for a long time to come.I have also benefited by the advice and guidance from **Dr. N.Sahu and Dr.J.K.Sahu** who also always kindly grant me their time even for answering some of my unintelligent questions about the project. I also gratefully thank all the employees especially the R&D members of OCL INDIA LTD, Rajgangpur for their help during the course of my project work.

I convey my heartfelt thanks and deep gratitude to my honorable teachers **Prof. J. Bera, Dr. R. Mazumder**, **Dr.S.Pal** and **Mr.A.choudhury** for their valuable advice, constant help, encouragement, inspiration and blessings.

Words fail me to express my gratitude to my family members who were always supporting me to do better improvement during the course of my journey in the Master degree.

Submitting this thesis would have been a Herculean job, without the constant help, encouragement, support and suggestions from my departmental brothers,especially **Y. Nayak**, **R. P.Rana**, **J.P.Nayak** and my loving friends **Sarat, Subrat**, **Ganga, Ganesh, Sunil, Shyama, Sanjaya, Niroj, Smruti** and younger brother **Bhabani** for their time to help.I would also express my sincere thanks to lab. members of Department of Ceramic Engineering, N.I.T., Rourkela. Above all, I thank almighty for giving me all these people to help and encourage me, and for the skills and opportunity to complete this thesis.

(Rashmi Ranjan Rout)

PREFACE

Chapter – 1 introduces the topic and background of the existing field. **Chapter – 2** deals with detailed literature review. Attempts have been made to systematically classify the available information under different sections. This chapter incorporates background information to assist in understanding the aims and results of this investigation, and also reviews recent reports by other investigators with which these results can be compared. The end of **Chapter – 3** deals with the objectives of the present investigation. **Chapter – 4** deals with the detailed experimental processes related to this research work. **Chapter – 5** deals with the results and discussion systematically with respect to processing, characterization, densification study and evaluation of thermo-mechanical properties. **Chapter – 6** summarizes the conclusions, whereas possibility of future work has been given after the conclusion.

A complete list of references has been given towards the end of the thesis.

ABSTRACT

Alumina-carbon (Al_2O_3-C) refractories are extensively used for steel making application particularly for continuous casting of steel owing to its high modulus of rupture and high cold crushing strength, low thermal expansion coefficient, high thermal conductivity, high thermal shock resistance and resistance to molten slag and metal. The effect of alumina aggregates on the physical, mechanical, thermal and thermo-chemical properties of Al_2O_3-C has been systematically studied in this present investigation. White fused alumina (WFA), brown fused alumina (BFA) and tabular alumina (TA) have been used as a source of alumina. Flakey graphite has been used as a source of carbon. Fused silica has been incorporated into the Al_2O_3-C composition in order to provide low thermal expansion coefficient of the Al_2O_3-C refractories. Phenolic resins were used as binder to bind the different aggregates of the Al_2O_3-C refractory formulation. Different Al_2O_3-C refractory formulation were prepared by varying the alumina aggregates (types) and amount keeping total alumina aggregate, fused silica aggregate, graphite and binder unaltered. Physical properties like apparent porosity (AP) and bulk density (BD), mechanical properties like cold modulus of rupture (CMOR), cold crushing strength (CCS), and modulus of elasticity (MOE), thermal expansion coefficient (TEC) and thermo-chemical properties like oxidation resistance and erosion resistance were studied as a function of alumina aggregate (amount and type) of the fired (1050^0C for 3 hr) Al_2O_3-C refractory samples. Although the alumina aggregate substitution showed a negligible variation in the physical properties of the Al_2O_3-C refractory it shows a substantial effect on the mechanical and thermo-chemical properties. The observed results has been correlated the aggregates type, morphology, (size, shape and distribution). An attempt has also been made to study the effect of metallic silicon antioxidant addition on the above properties were studied as a function of alumina aggregate type.

Table of Contents

List of Figures

Abbreviations

AP-Apparent Porosity

BD-Bulk Density

MOR-Modulus of Rupture

CCS-Cold Crushing Strength

TEC-Thermal Expansion Coefficient

MOE-Modulus of Elasticity

WFA-White Fused Alumina

BFA-Brown Fused Alumina

TA-Tabular Alumina

CHAPTER 1

Chapter-1 Introduction

1.1 General Information

Refractories, a key input for iron and steel making, assume ever increasing role due to high stress on production of high quality sophisticated steels, which alone accounts for the consumption of nearly 70% of total refractories produced [1]. Refractories in general, are the non-metallic materials that are hard to melt at high temperature and having enough mechanical strength and heat resistance to withstand rapid temperature change, including repeated heating and cooling and resistance to molten slag and metals. Generally refractories are classified into two categories i.e.(i) the shaped refractories, available in the form of different brick shapes, and includes the oxide and non-oxide system (ii) the unshaped refractories, which includes mortars, castables, plastics etc.[2]. In recent years, in tune with the changing trends in steelmaking, especially continuous casting and ladle metallurgy, the demand for high performing shaped refractories are on an increasing demand. The higher campaign lives and the variability of newer steel making operations are decided by the availability and performance of such shaped refractories with superior high-temperature strength, erosion and corrosion resistance. The composite refractories that consist of elemental oxides and carbon (Al_2O_3-C, MgO-C, ZrO_2-C etc.) have found more importance due to their superior thermo-mechanical and thermo-chemical properties. These kinds of refractories have the importance in iron and steel sector due to their excellent performances in different application areas e.g. lining in electric arc furnace (slag zone and striking pad)ladles and converters (slag zone, charge pad, tapping belly etc.), casting nozzle, sliding gate plates, etc. Among the several carbon containing refractories,Al_2O_3-C refractories have been developed subsequently for the improvement in the steel quality i.e in particular for continuous casting of steel.[3]

1.2 Advantages of Al_2O_3-C Refractories

The advantages of Al_2O_3-C refractories are given as listed below:-

- High Flexural and compressive strength
- Low modulus of elasticity

- High thermal conductivity
- Low thermal expansion
- High thermal shock resistance
- Resistance to molten metal and slag

1.3 Problems Occurring in Al_2O_3-C refractories

In spite of above advantageous properties, alumina-carbon refractories have been facing the problems, particularly the wear of the refractory components, which can simply be described with a three-step process:-

- Oxidation of carbon at temperature above 600°C which leads to the deterioration of properties in refractories i.e. increase of porosity, decrease of strength and corrosion resistance.
- Erosion (chemical or physical) by penetration of molten metal or slag in the pores or due to the dissolution of alumina by slag or the oxidation of carbon by iron oxide in liquid slag and ambient gas.
- Direct wear by liquid iron flow and thermal or mechanical spalling.

1.4 Solutions to the problems

- Use of antioxidants play an important role for reducing oxidation of carbon.
- Use of high purity raw materials that reduce the erosion or corrosion properties.

1.5 Raw Materials For the Al_2O_3-C Refractories

The raw materials used for Al_2O_3-C refractory manufacturing are the aggregates consisting of alumina (fused and/or sintered) and fused silica, flaky graphite, binder (phenolic resins) and antioxidants (metallic Si and/or Al powder, or nonmetallic SiC).

1.5.1 Role Of Alumina Aggregates

Different alumina aggregates, in general fused and sintered alumina have been used for the processing of the alumina-carbon refractories. White fused alumina (WFA) and brown fused alumina (BFA) were coming under the fused alumina category and tabular alumina(TA) is under sintered category. It has been reported that the properties of Al_2O_3-C refractory is influenced by the type of alumina aggregates.

*1.5.1.1 General Idea About Alumina Aggregate*s

White fused alumina (WFA) are the pure form (>99% Al_2O_3) of fused alumina, having high refractoriness, abrasion resistance or chemical inertness but they have more porous or lower bulk density in the product. Brown fused alumina (BFA) are basically impure (~95% Al_2O_3) but extremely dense material, high abrasion resistance. The tabular alumina is highly chemical pure (>99% Al_2O_3) and has high particle density. The materials have excellent volume stability and chemical inertness.

1.5.1.2 Grain Morphology Of Alumina Aggregates

Although the total porosity of white fused alumina is similar to the tabular alumina, it contains mainly large interconnecting open micropores. The crushing strength of white fused alumina is lower than that of brown fused alumina and tabular alumina. The porosities present in tabular alumina are spherical closed pores only. The open porosity of white fused alumina is three times higher than that of tabular alumina. The presence of evenly distributed closed pores in tabular alumina contributes to the low water absorption. An excessive open porosity would also result in greatly differing grain strength and high temperature volume stability. Partially sintered grains would exhibit poor volume stability and shrink further when used at high temperature. Although higher density has been found in brown fused alumina, the thermal shock resistance of brown fused alumina reduces due to lack of closed porosity. The presence of TiO_2 in brown fused alumina leads to higher densification. But liquid phase sintering would already appear at higher temperature, which results in degradation of high temperature properties. The thermal spalling resistance of tabular alumina is very high due to the presence of closed porosity. The spherical closed pores act as inhibiter to crack propagation during thermal cycling [4]. The rough and

irregular shape surface morphology of tabular alumina aggregates provides better interlocking with other aggregates and shows better mechanical strength. In contrast, the fused alumina aggregates grain shows smooth surface resulting lower mechanical strength in comparison to the sintered alumina.[5]

1.5.2 Role of Carbon

Flaky graphite is used as a source of carbon in the manufacturing of Al_2O_3-C refractories due to its following properties:-

- High melting temperature
- High thermal conductivity
- Low thermal expansion coefficient
- High thermal shock resistance
- Low friction and hence good compressibility character
- Low wettability to molten slag and hence better corrosion or erosion resistance
- Good oxidation resistance. It starts to be oxidized in oxidizing atmosphere at (500°C)

1.5.3 Role Of Fused Silica

Fused silica is used as refractory aggregates in Al_2O_3-C refractory in order to reduce the thermal expansion coefficient of Al_2O_3-C refractory. It also reacts with the alumina at high temperature and forms mullite which provides better interlocking structure and imparts better high temperature strength. The amorphous nature of fused silica has a disadvantage of forming low melting compound with the other aggregates of the refractory, which leads to deterioration of high temperature properties of the alumina-carbon refractory.

1.5.4 Role Of Binder

The main role of binder is to provide green strength to ceramic bodies. In addition to this cohesive action, selection of binders usually involves consideration accompanying characteristics of the aggregates. Generally Phenolic resins have been used as binder for the Al_2O_3-C refractories as they can be pyrolysed during coking to achieve a high carbon yield about 55- 65% of their solid content as carbon. The phenolic resin provides better carbon bonding & compatibility with other carbonaceous materials but it has the disadvantage of lower oxidation resistance than other binders like pitch.[6]

1.5.5 Role Of Antioxidant

The antioxidant (usually additives) plays important role in alumina –carbon refractories in the context of oxidation protection of carbon bonds. The function of antioxidant is given as below:-

- They themselves melt or form low melting glassy phase and coats the carbon bonds to protect them from being oxidized.
- Get oxidized and reduce the partial pressure of oxygen available to oxidize the carbon bonds.

However, the addition of antioxidants should be optimized to make a balance between the properties of oxidation and corrosion resistance. Generally, metallic silicon, aluminium powder or nonmetallic carbides such as SiC were used as antioxidants (or additives) in the Al_2O_3-C refractories to improve the physical and thermo-mechanical properties.

1.5.6 Application Areas Of Al_2O_3-C Refractories

Alumina–Carbon refractory has made up of a significant proportion of refractories. Few application areas for the alumina-carbon refractories in the iron and steel sector are given as below:-

- Striking Pad and Slag Zone of Transfer Ladle
- Lining of Blast furnace
- Sliding plate for Ladle
- Continuous casting of steel (Shrouds, Immersion nozzles)

In most of the literature, it was found that the variation in different alumina aggregates, either brown fused, white fused or tabular alumina influence the physical, thermo-mechanical as well as thermo-chemical properties.[7] Most of the literatures have been focusing the properties and performance of alumina-carbon refractories on the basis of different alumina aggregates like white fused alumina (WFA) or brown fused alumina (BFA) or tabular alumina (TA). Very few literatures have reported the combined effect of alumina aggregates (type and amount) on the properties of the Al_2O_3-C refractories. The present research work aims to study the effect of different substitution of alumina aggregates on the physical properties like apparent porosity (AP) and bulk density (BD), mechanical properties like cold modulus of rupture (CMOR), cold crushing strength (CCS), and modulus of elasticity (MOE), thermal expansion coefficient (TEC) and thermo-chemical properties like oxidation resistance and erosion resistance of Al_2O_3-C refractory. Different Al_2O_3-C refractory formulation were prepared by varying the alumina aggregates (types) and amount keeping total alumina aggregate, fused silica aggregate, graphite and binder unaltered.

CHAPTER 2

Chapter-2 *Literature Review*

The literature review is divided into four major sections. Section 2.1 to 2.2 provide necessary information about the effect of additives on carbon containing refractories basically Al_2O_3-C and MgO-C. Section 2.3 to 2.6 reviews the thermochemical effect on the above refractories and section 2.7 to 2.8 describes the effect the graphite,the binder and different atmosphere effect on the properties carbon containing refractories.This chapter incorporates background information to assist in understanding the aims and results of this investigation, and also reviews recent reports by other investigators with which these results can be compared.

2.1 Effect of Additives on the Mechanical and Thermochemical Properties of Al_2O_3-C Refractory

Javadpour J. *et al*. [8] have studied the effect of Al and Si additions on the properties and microstructure of Al_2O_3-C refractories. It has been observed that the strength increases and porosity decreases with increase in the Al as well as Si content in the samples. This improvement was due to the formation Al_4C_3 and AlN phases in the Al containing samples and SiC formation in case of Si containing samples. It has also been reported that the improvement in the properties are sensitive to firing temperature in case of Al additive but not for Si additive. For example the strength was found to decrease with increase in firing temperature in case of Al containing sample and the same was found to increase in Si containing samples. The lowering in strength with increase in firing temperature in Al containing sample has been attributed to the decrease in the amount of Al_4C_3 phase with the increase in the firing temperature. The oxidation resistance was reported to improve with both Al (0-5 wt%) as well as Si (0-5wt%) additives. However, the formation of SiO_2 layer at the surface limits the improvement in the oxidation resistance at higher percentage of Si addition.

The effect of combined addition of aluminum and silicon metal powder on the performance and properties of alumina graphite composite refractories have been studied by Guoqi, Liu ***.et al.*** [9]. It has been reported that the weight loss for the sample without metal additive was less than that

with metal additive, when heat-treated at same temperature. The weight loss of the sample with metal additive was found to decrease with heat treating temperature. The strength of sample with additives was higher than that without additives and was found to decrease slowly above 1200^0C.The bulk density of the sample with additives was higher (lower apparent porosity) than that of sample without additives which was found to increase with increase in temperature. This is due to the in-situ AlN and a little Al_4C_3 formation when the heat-treated temperature above 1200^0C. The formation of Al_4SiC_4 in the samples containing both the additives leads to the increase in strength when fired above 1300^oC.

Shaowei , Z. *et al*. [10] have studied on the behavior and effects of antioxidants like $Al_8B_4C_7$ and Al_4SiC_4 on the carbon containing Al_2O_3-C refractories. It has been reported that $Al_8B_4C_7$ and Al_4SiC_4 showed an excellent oxidation resistance. This is due to the fact that when $Al_8B_4C_7$ added to carbon-containing refractory, it reacts with $CO_{(g)}$to form Al_2O_3 and B_2O_3 which further react with each other to form liquid phase from low temperatures. The liquid phase forms a protective layer on the surfaces of the refractory and thus inhibits the oxidation of the refractory. However, this effect of $Al_8B_4C_7$ as an antioxidant decreases at high temperature, owing to the evaporation of B_2O_3. On the other hand Al_4SiC_4 forms protective layer (Al_2O_3-SiO_2) on the surfaces of the refractory as Al_4SiC_4 reacts with CO(g)) and thus inhibits oxidation.

Bernard Argent B. *et al*. [11] have studied on the effect of additives (5% Al, 10% Si, 5% B_4C & 5% BN, 5% B_20_3, and 15% Si_3N_4) on the slag resistance of $A1_20_3$-SiO_2-SiC-C refractories in Air. A fairly good wear resistance was observed with the predicted content of SiC in the refractory in the as-fired condition. The most effective additives were found to be silicon and B_4C, whilst the most deleterious was B_2O_3 as slag resistance is concerned. These results were interpreted in terms of the thermo chemical predictions, including the variation in oxygen potential with slag attack. This study enables one to rank the refractories in order of likely resistance to attack - large amounts of liquid in the as-fired state favoring attack and reported that large amounts of SiC associated with Si additions and large amounts of BN associated with B_4C additions favored resistance to attack. Although the predictions about the order of oxidation of C and SiC were found correct for iron oxide-free slag, they were found wrong for refractories other than those with silicon-containing additions exposed to iron oxide-bearing slag. This was due to the slow rate of oxidation of SiC at low oxygen activities.

The effect of ZrO_2-SiC composite on the oxidation resistance of Al_2O_3-C refractory have been studied by Jingkun,Yu. *et al.* [12]. The phase composition and microstructure of the synthesized composite were investigated by XRD and SEM. It has been found that the increase in heat treatment temperature promotes the synthesis of ZrO_2-SiC composite. The optimized temperature to synthesize the composite was 1873 K. It has been reported that the addition of synthesized composite had improved the oxidation resistance of the Al_2O_3-C refractory and the refractory with 6% (ZrO_2-SiC) addition had the best oxidation resistance.

2.2 Effect of Additives on the Physical, Mechanical and Thermo chemical Properties of MgO-C refractory

The effect of TiO_2 and TiO_2/Al addition in MgO-C refractories has been investigated by Hub´alkov J. *et al*. [13]. The formation of TiCN and TiC compounds in the samples containing TiO_2 and TiO_2/Al additives was reported to be responsible for the improved oxidation resistance, mechanical strength as well as the abrasion resistance of the bonding matrix. The additionTiO_2 in carbon-bonded refractories with Al as an antioxidant, contributed to the formation of mainly crystalline Al_4C_3, Al_2OC and Al_4O_4C dumbbell shaped whiskers. These whiskers have a higher oxidation resistance in comparison to amorphous whiskers containing Al, C and O and increase the thermal shock resistance due to interlocking in the bonding matrix. Micostructural study revealed the presence of AlN only at the interface carbon matrix/Al-grain.

Gurcan, C. *et al*. [14] have studied the effect of various antioxidants namely Al, Si, SiC and B_4C on the oxidation resistance of magnesia–carbon bricks in the temperatures ranges 1300^0C-1500^0C. B_4C was found to be the most effective and SiC was found to be least effective antioxidants in the studied temperature range. The formation of the impermeable dense $Mg_3B_2O_6$ layer on the brick surface was found when fired at 1500^0C. Magnesium–borate, which is in liquid state above 1360^0C, had an excellent effect on the oxidation resistance of the bricks by filling up the open pores and forming a protective layer on the surface. Forsterite (Mg_2SiO_4) and Spinel ($MgAl_2O_4$) provided similar effects when metallic Si and Al added as antioxidant respectively. Volume expansion and cracks were observed in MgO–C refractories containing 3% Al, oxidized at 1300^0C, but were rarely seen in the Al added specimens oxidized at 1500^0C.

These physical changes were the results of hydration of Al_4C_3 .The SiC added specimens had similar phases with Si added specimens,but least effective one as because of the formation of a lower amount of forsterite phase in the SiC added bricks compared to the Si added bricks.

The effect of ferrosilicon-silicon antioxidant on the properties of magnesia-graphite refractory has been studied by Nemati Z, A. *et al*. [15]. It has been observed that the ferrosilicon-silicon containing specimens showed the least apparent porosity with increase of temperature in comparison with samples containing silicon or ferrosilicon alone. The ferrosilicon-silicon containing specimens showed more CCS and MOR with increase of temperature than silicon or ferrosilicon containing specimens. The formation of phases such as forsterite and magnesio-ferrite and their volume expansion (in the ferrosilicon-silicon containing specimens) are the main reasons for more compact structure, filling of the pores, decrease of porosity and permeability. Consequently oxidation resistances of the ferrosilicon-silicon containing samples are more than silicon or ferrosilicon containing specimens. The best results were obtained for the samples containing 1-3 wt. % silicon and 2-4 wt. %. ferrosilicon.

Krivokorytov, E. V. *et al*. [16] have studied on the effect of antioxidants on the properties of unfired carbon bearing refractories i.e. periclase-carbon and aluminum-periclase-carbon refractories. It has been observed that the introduction of aluminum and crystalline silicon into the composition of the refractory mixture decreased the degree of burning-out in 3-h heat treatment at 1200^0C. The thermo reactive binder based on a resorcinol oligomer used for the production of refractory specimens was found to have a favorable effect on the preservation of carbon in the refractory due to the activation of the oxidation of the coke formed in polymerization of the oligomer. The study suggests that these factors should improve the slag- and metal-resistance of the refractory.

The behavior of Al_4SiC_4 addition to the MgO-C refractories has been studied by Hoshiyama,Y. *et al*. [17]. It been observed that the density increases and the porosity decreases in the MgO-C brick on addition of Al_4SiC_4 powder above 1000ºC. The apparent porosity after heating at 1500ºC was found 2% lower than that after heating at 800ºC. The brick strength was increased gradually above 1000ºC by the addition of Al_4SiC_4 powder. Al_4SiC_4 powder has improved the

oxidation resistance of the bricks. The bricks containing Al_4SiC_4 had high slaking resistance after heating. Al_4SiC_4 reacts with CO gas to form spinel ($MgAl_2O_4$) and SiC above 1200ºC. The formed SiC also reacted with CO gas and MgO to form forsterite (Mg_2SiO_4) above 1400ºC. Al_4C_3 and AlN were not formed in these reaction processes.

2.3 Dissolution Mechanism of Alumina Aggregates in Molten Slag

Kryvoruchko P. *et al*. [18] have made a comparative study of the properties like apparent porosity, bulk density, cold crushing strength, refractoriness under load, linear shrinkage, creep & thermal shock resistance between different alumina i.e. fused and sintered. They found that the sintered and white fused alumina are practically equivalent materials for production of alumina refractories with good properties of purity, open porosity, apparent density, cold crushing strength and refractoriness under load. However, the refractory of sintered alumina has higher thermal shock resistance, whereas refractory of white fused alumina has higher creep resistance. Both types of refractories have similar interaction with melted steel.

The dissolution and settling of spherical alumina particles into the synthetic slag of various compositions in the temperatures 1200^0 and 1400^0C have been studied by Sridhar S. *et al*. [19]. It was observed that the surface remains smooth and no reaction layer was formed when the slag was without or contains low FeOx. The dissolution curves indicate that the dissolution process was controlled by the diffusion of species. The total dissolution times of spherical particles in slag A (0 % FeOx) , B (5% FeOx) and C (9% FeOx), at 1400^0C, are 3150, 1440 and 944 s, respectively. At 1200^0C, there is no appreciable dissolution observable due to the fact that the slag was saturated with Al_2O_3.

Liu, J. *et al*. [20] have studied on the dissolution of alumina spheres in a synthetic $CaO–Al_2O_3–SiO_2$ (CAS) slag in the temperature range between 1470^0Cand 1630^0C. It has been observed that the use of spherical particles was shown to increase the experimental resolution of the dissolution phenomenon, and consequently the determination of the dissolution mechanism was more convincing. The driving force for Al_2O_3 dissolution was related to the concentration difference of Al_2O_3 between the particle/slag interface and the bulk of the slag. Mathematical simulations

showed that the dissolution mechanism was diffusion controlled, yielding an excellent agreement with the experimental data. The diffusion coefficients have been obtained ranging from $2.4*10^{-11}$ to $9.7*10^{-11}$ m^2/s in the temperature range between 1470^0C and 1630^0C.

2.4 Erosion or Corrosion in Al_2O_3-C refractory

Zhang ,S. *et al*. [21] have investigated on the dissolution mechanism of commercial white fused alumina (WFA) and tabular Al_2O_3 (TA) grains into a model silicate slag. It has been reported that the dissolution of WFA grains in the slag was higher than the TA grains tested at different temperature. The formation of CA_6 and hercynitic spinel layers was found at Al_2O_3/slag interfaces. Liquid present in the CA_6 layer adjacent to the WFA at 1450°C provides an easy transport path for ions and thus increases the extent of direct dissolution. However, a thick, continuous and liquid-free CA_6 layer was formed adjacent to the WFA at 1600°C. Thus the dissolution of WFA became fully indirect at this temperature, requiring mass transport through the CA_6 interlayer to access the Al_2O_3. The CA_6 and spinel layer that formed adjacent to the TA was not continuous at both temperatures, and hence TA dissolution was never fully indirect. In these samples the slag could penetrate readily to the grain interior via grain boundaries. Hence TA grains were directly corroded and disintegrated by the penetrating slag in these samples. After the formation of CA_6 and spinel, the remaining cations in the boundary layer formed low-melting phases, which dissolved into the slag at high test temperature. These phases (anorthite solid-solution needles and hercynitic spinel dendrites) precipitate during cooling from the test temperature.

The corrosion resistance and microstructure of Al_2O_3-C based refractories have been studied by Qingcai Liu *et al*. [22] in smelting reduction melts by the quasi-stationary immersion and rotary immersion test. They reported that the corrosion rate of the Al_2O_3-C (AC) based refractories was decreased with the addition of the graphitic carbon and ZrO_2. The test results showed that the ZrO_2 containing bricks (AZ) had much better corrosion resistance than the ZrO_2-free bricks. The ZrO_2 addition improved the oxidation resistance of the refractory and decreased the interaction rate between the melts and the refractory. The corrosion of the Al_2O_3-C based refractories is caused by the interaction between melts and refractory, and the dissolution of the refractory

constituents into the melts. The corrosion rate of both AC and AZ system refractories was found to increase with the iron oxide content of the melts and the temperature of the molten bath. The corrosion rate of the rotary test was 30% higher than that of quasi-stationary immersion test. The corrosion mechanism of AC refractories in the smelting reduction melts with iron bath was deteriorative layer formation followed by graphite oxidation. The interaction between melts and refractory and the dissolution of the refractory constituents into the melts governs the corrosion for the AZ refractory. The microstructural study revealed that the new compounds $FeSiO_3$, $ZrSiO_4$, Ca_3FeO_4, $CaSiO_3$ were formed in the deteriorative layer during the interaction between the melts and AZ refractory system.

Zhao, L. *et al***.** [23] have studied the interfacial phenomena during the interaction of liquid iron and graphite/alumina mixtures. It has been reported that the carbon dissolution strongly depends on the wetting/non-wetting behavior of the refractory/molten metal interface or in the other wards the contact angle of the liquid iron - refractory interface. It has been observed that during the graphite/iron interactions, the contact angle changed from 64° at the initial state to 38° at the final state and thus showed a good wettability between iron and graphite. However, addition of different amounts of alumina into the graphite substrate caused the contact angle to increase. When the alumina in the substrate increased from 16.7 to 23.1%, the contact angle demonstrated a sharp change from good wetting to almost non-wetting. A fairy high rate of carbon dissolution was observed when the contact angle was low (at low alumina content) on the other hand it decreases sharply when the alumina in the substrate increased from 16.7 to 23.1%. This decrease rate of carbon dissolution has been attributed to the poor wetting behavior of graphite/alumina substrate.

The interaction between slag- Al_2O_3-SiC-SiO_2-C refractory has been investigated by Hong, Lan. *et al.* [24]. The composition of the slag and refractory studied in this investigation were 45.4% SiO_2 - 36.6% CaO - 15.9% Al_2O_3 and 69.4% Al_2O_3 - 7.3 % SiO_2 - 10.6 % SiC - 12.7 % C respectively. The slag refractory interaction has been studied in the temperature range 1773 to 1873 K. XRD study confirmed that the formation of mullite when the refractory samples were maintained at high temperatures. The refractory/slag reaction has been evaluated from the carbon dissolution of the refractory. The time dependence carbon dissolution from the refractory was

found to follow a two step process. During the initial stage the carbon dissolution rate was high and then it is decreased. The high carbon dissolution from the refractory has been correlated with the evolved gases. The gas chromatographic analysis study confirmed the evolution of both CO and CO_2 gases during the initial stage however the latter disappeared as the time increased. The main *in-situ* reaction product was SiC rather than SiO. Slag showed a good wetting with the refractory and penetrated into the refractory through pores. The formation of low melting compounds like anorthite ($CaAl_2Si_2O_8$) and gehlenite ($Ca_2Al_2SiO_7$) were confirmed at the slag refractory interface when heated for a longer time.

The role of ash impurities in the depletion of carbon from the alumina-graphite refractory into liquid iron have been investigated by Khanna, R. *et al.* [25] Two natural graphite, containing 2.1% (NG1) and 5.26% ash (NG2) were used in this study. The carbon pick-up by liquid iron from alumina–natural graphite has been measured at 1550°C by a sessile drop arrangement. and was compared with the carbon pick-up from alumina–synthetic graphite mixtures. It has been observed that both natural graphite under investigation, showed high level of carbon dissolution into liquid iron. The presence of up to 30% alumina had negligible effect on carbon dissolution from alumina–natural graphite refractories with carbon concentration in the melt reaching 5 wt%. However a significant reduction in carbon dissolution was observed for alumina in the concentration range 30 to 40 wt%. Further it was observed that the significant differences in ash composition of the natural graphite used under this investigation leads to the difference in the nature of deposits observed in the interfacial region. While a small number of sporadic deposits were observed in the case of alumina–NG1 mixtures, a layer of fused ash appeared to cover the interfacial region in case of NG2. However in both cases, EDS analysis of the interfacial region indicated the presence of Ca, Mg, Al, Fe, O and S in close vicinity. It was therefore confirmed that alumina in the refractory interacts with various oxides present in the ash impurities.

Sasai, K. *et al.* [26] have investigated the reaction kinetics between silica-containing alumina-graphite refractory and low carbon molten steel. The study suggested that the rate of reaction between the refractory and the molten steel was controlled by diffusion of the SiO gas and CO gas through the pores of oxide film formed at the refractory-molten steel interface. The rate of the reaction between the refractory and the molten steel was found to be dependent on steel

grade. For example the reaction was found faster in the Ti-killed molten steel than in the Al-killed molten steel. This steel grade dependence had been ascribed to the differences in the gas permeability through the oxide film formed at the refractory-molten steel interface. In other words, the surface of the refractory immersed in the Al-killed molten steel was nearly covered with a relative dense oxide film present in both solid and liquid phases, whereas the surface of the refractory immersed in the Ti-killed molten steel was discontinuously covered with a relative porous oxide film in the solid phase.

2.5 Erosion or Corrosion in MgO-C refractory

The corrosion in magnesia-carbon refractory have been studied by Sunayama, H. *et al.* [27] rotating the cylindrical samples in molten slag at 1673K. It has been reported that the corrosion behavior was affected by the slag composition. The decrease of corrosion rate was found with decrease in MgO content of the slag. The rotation speed did not have any significant effect on the corrosion rate. It has been suggested that the movement of CO bubble through the boundary layer strongly affect the dissolution rate of MgO grains. The study suggests that the reduced rate of CO bubble formation is effective to improve the corrosion resistance of MgO-C refractory in molten slag.

Li ,Zushu. *et al.* [28] have studied the behavior of MgO-C refractory with slag-metal system. It has been reported that the reactions between MgO-C refractory with slag-metal was due to the dissolution of MgO and graphite in the refractory into slag and metal respectively. It has also been reported that the generation of gas bubbles was responsible for the corrosion. The local corrosion was regarded as due to the cyclic dissolution of MgO and graphite in the refractory into slag and metal phase respectively. The study suggests that gas bubbles formed mainly according to the reaction between (FeO) in slag film and C(s) in the refractory by the reaction (FeO) + C(s) = Fe(l) + CO(g). The corrosion rate was found to be influenced by the bubble generation position and the number of bubbles generated. Bubbles generated in the three-phase boundary restrain the local corrosion, while bubbles generated at the refractory metal interface enhance the local corrosion.

Zhang, S. *et al.* [29] have investigated the influence of additives on the corrosion resistance and corroded microstructures of MgO–C refractories in a model EAF slag (CaO/SiO_2 weight ratio = 1.38) for 30 h at 1650^0C. It has been reported that Al additions improved C oxidation resistance at 1650^0C only a little, but accelerated MgO dissolution resulted in a minor effect on corrosion resistance. Additions of Si or Al+Si was found to improve C oxidation resistance slightly but accelerated MgO dissolution more as compared to Al additions thus, resulted in worse corrosion resistance than Al addition and no addition. B_4C showed the worst corrosion resistance due to formation of boron containing liquid in the refractory which greatly accelerated MgO dissolution, resulting in C in the matrix, which easily eroded by the slag. With double addition of $Al+B_4C$, boron-containing liquid formed, which not only inhibited effectively C oxidation, but also accelerated formation and growth of $MgAl_2O_4$ spinel (MA) crystals between graphite in the matrix at the test temperature. The formation of MA provides the integrity of the refractory texture, and thus best corrosion resistance was observed in the $Al+B_4C$ containing refractory.

Lee W.E *et al*. [30] have studied on the penetration and corrosion resistance of high purity sintered and fused magnesia grain by model EAF (CaO/SiO_2 = 1·38) and BOF slag (CaO/SiO_2 = 3·29) at 1600 and 1700°C. It has been found that at the test temperatures, Fe and Mn ions from both model slag were diffused into the magnesia grain to form magnesio-wustite, (Mg,Fe,Mn)O. The magnesio-wustite formed adjacent to the slag had a much larger crystal size than that of the bulk MgO far from the MgO/slag interface. The large magnesio-wustite grains limit the potential for grain boundary penetration into the sintered magnesia. The magnesio-wustite layer formed with the EAF slag took up more Fe_xO from the slag than that formed with the BOF slag, which was partially responsible for a lower slag penetration into sintered magnesia grain since the remaining silica rich local liquid was rendered more viscosity. It has also been reported that the EAF slag was not saturated with respect to MgO, so the magnesio-wustite which formed later reacted with Ca and Si ions remaining at the MgO/EAF slag interface to form low melting phases such as merwinite (C_3MS_2) and then dissolved into the slag, rendering the dissolution process essentially indirect.

2.6 Erosion or Corrosion in Carbon Containing Composite Refractories

Baldo,J.B. *et al*.[31] have studied on the corrosion resistance of resin bonded alumina/magnesia /graphite refractories containing different kinds of aggregates subjected to the action of slag of several CaO/SiO_2 ratios. They also investigated the influence of alumina/carbon ratio and magnesia and silica contents on the refractories corrosion resistance. It has been observed that as the graphite content was high enough (6 wt%) to give good sinterability and small enough not to hinder the diffusion of ions responsible for the spinel formation. Lower concentration of the mullite phase resulted in a smaller production of calcium alumino silicates (eutectic composition anorthite-gehlenite MP.1265^0C). Higher periclase/mullite ratios resulted in higher mullite consumption due to its reaction with periclase, producing the forsterite ($2MgO.SiO_2$) phase and alumina. This precipitated, highly reactive alumina was able to combine with the excess of periclase, forming initially magnesium aluminate and later magnesium-aluminum Spinel ($MgAl_2O_4$). The study suggested that the combined effect of these reactions in the refractory microstructure creates barriers in the open porosity originating a concurrent mechanism of protection. The use of electrofused alumina in substitution to sintered alumina and bauxite in the formulations promoted an increase in the corrosion resistance as a consequence of the smaller rate of dissolution by the slag. In this case the A/C ratio was 12.9.

The properties and corrosion of alumina-magnesia-carbon refractories have been studied by Pötschke,J. *et al*. [32] . The content of the mixture contains magnesia 5 - 35 % and the carbon content about 10 %. Coking of the "as delivered bricks" has resulted in an increase by about 6 % of porosity, and on firing at 1250°C it was about 8 %. The burning-out of 10 % carbon has raised porosity by about 15 % in the samples. The porosities of the oxidized fired bricks at 1250°C have the range between 24 - 30 %. A post-firing expansion of the AMC refractory was observed due to the formation of spinel at high temperature. The post-firing expansion becomes stronger with higher contents of MgO and in a reducing atmosphere. The decarburisation of AMC-refractories in air was found to be controlled by the diffusion of oxygen in the open porosity. A slag layer on the refractory surface has been found by laboratory tests and practically resulted best protection for preventing oxygen diffusion. The metallurgical corrosion resistance of bauxite based AMC-refractories has been found to be poor as compared to alumina based ones.

2.7 Effect of Atmosphere on the Carbon Containing Refractories

Bavand-Vandchali, M. *et al*. [33] have investigated the effects of carbon, air and reducing atmospheres on microstructure and phase evolution of in situ $MgAl_2O_4$ spinel formation in the matrix of MgO–C refractories. It has been reported that the formation of spinel was started under 1000^0C in both air and reducing atmospheres. The study suggested that the solid-state reaction was the dominant mechanism of spinel formation in oxide atmosphere, while the gas–solid reaction was found to play a vital role in reducing atmosphere. Reaction of MgO and C in reducing atmosphere led to the formation of Mg(g) which was found to be partially controlling the in situ spinel formation in the carbon containing samples fired in reducing environment. The in situ spinel formation was due to reaction of reactive alumina and magnesia initiated around 1000^0C in both reducing and oxidizing atmospheres. This reaction was completed above 1450^0C where no signatures of the corundum peaks were found. The partial pressure of Mg(g) originated from MgO reduction was found to have an important role on the in situ spinel formation. The intermediate phases such as CA_6 were clarified to be formed due to reaction of MgO impurities with reactive alumina at 1450^0C. The low-melting CMAS phases was also formed in triple junction of spinel, which was believed to be responsible for corrosion resistance decrease at high temperatures. The nature of spinel in MgO–C refractories matrix produces an interlocking texture, which holds the graphite flakes within and improves the structural integrity. In this type of skeleton structure, the graphite and antioxidants can be confidently increased for getting better wear resistance and with less negative effects on properties of MgO–C refractories.

Ghosh N,K .*et al*.[34] have investigated on the oxidation mechanism of MgO-C refractories containing 20wt % graphite in air at various temperature (from 800^0C to 1600^0C). It was found that the rate of decarburization increased with rise in temperature from 800^0C to 1400^0C and then remained more or less constant from 1400^0C to 1600^0C. The reaction rate was found to be controlled by diffusion of oxygen through the decarburized layer. At higher temperature (> 1400^0C), oxidation of graphite takes place indirectly by the reaction $MgO(s) + C(s) \rightarrow Mg(g) + CO(g)$. The magnesium vapour thus produced is deoxidized at the outer surface and redeposited

as MgO. This leads to a reduction in porosity in the decarburized outer shell and consequently a reduction in the rate of oxidation.

Guoqi Liu *et al*. [35] have studied on the influence of heat-treatment atmosphere (argon, $CO+N_2$ and nitrogen) on Al_2O_3-C (AG) samples with metallic Al addition. The study suggested that none of these three heat-treating atmospheres can avoid the formation of Al_4C_3. However, different heat-treatment atmosphere can influence the hydration resistance of the samples containing metallic Al. The hydration resistance of the material heat-treated in N_2 atmosphere was found to be the best. Microstructural study suggests the formation of sub micrometer whiskers shaped Al_4C_3 when heat treated under $C+N_2$ atmosphere. On the other hand, formation of floccules, band shaped and hexagonal coniform like whiskers and granular AlN was observed when the samples were heat treated under Ar and N_2 atmosphere respectively. Heat-treatment in $C+N_2$ and N_2 were found beneficial to increase the strength and decrease the apparent porosity of the samples with metallic Al addition.

2.8 Effect of Resin and Graphite on Carbon Containing Refractories

The effects of resin type and content as well as graphite content on physical and mechanical properties of MgO-C refractories have been studied by Nemati,Z.A. *et al*. [36]. It has been reported that, the low-viscosity resins improved compressibility however the strength is degraded. Higher resin content was found to improve the compressibility, but it caused higher porosity after preheating at 600^0C. The results also showed that the porosity and density of tempered samples were decreased on increasing the graphite content. It has been found that the porosity decreased when the resin content increases in the tempered samples. This effect was due to the improvement of compaction during pressing as resin content increases. However, in the preheated samples at 600^0C, the porosity was found to increase when the resin content increases, which reported to be resulted from burning out of total organic portion of resin (about 70 wt.%). On the other hand, cold crushing strength of the tempered (tempered at 240^oC) samples was found to increase when their resin content increases, due to decrease of porosity and improvement of resin bonds. Weight loss was found to increase with respect to time and temperature of oxidation test in the samples containing high amount of graphite.

Ivashchenko L. V. *et al*. [37] have studied the effect of graphite on the properties of periclase-carbon composite using graphite flake and elementary carbon. It has been observed that the open porosity of the specimens held for 1day after compaction was virtually independent of the type and the quantity of graphite. The ultimate compressive strength was found to decrease with increasing the graphite content and was 1.5-2 times higher in the case of the specimens containing graphite flake (have decreased gas permeability). The specimens containing flake graphite exhibit the best property after drying at 20^0C for a period of 24 h. A similar dependence of the open porosity, the strength, and the gas permeability of the specimens on the content and the type of graphite was observed after heat treating at 1000^0C. A comparison of the gas permeability of the specimens before and after firing at 1000^0C showed that it was virtually identical, i.e., pores were evidently isolated (not interconnected) and decarbonization (carbon burn up) occurs only for the surface of the specimens. The specimens containing graphite flake showed better properties on heat treating at 1000^0C.

CHAPTER 3

OBJECTIVE

Al_2O_3-C refractories finds its application in iron and steel industries due to its superior properties like high strength, low thermal expansion coefficient, low modulus of elasticity, high resistance to chemical attack and high thermal shock resistance. Al_2O_3-C refractories are manufactured with aggregates (consisting of fused or sintered alumina, fused silica), flaky graphite bonded by phenolic resins with antioxidants (metallic Si and/or Al, and metal carbides SiC, Al) .The above mentioned properties of Al_2O_3-C refractory have been found to be dependent on the alumina aggregates type. For example Al_2O_3-C refractory prepared with tabular alumina shows higher thermal shock resistance than that prepared with fused alumina. However, a few of the literature have mentioned the combined effect of alumina aggregates (types) on the properties of alumina-carbon refractories. The intention of the thesis work is to systematically study the effect of alumina aggregates on the physical, mechanical, thermal and thermo-chemical properties of Al_2O_3-C refractories. The specific objectives of the present work are summarized below

(i) Formulation of Al_2O_3-C refractory by varying the alumina aggregates (types and amount) keeping total alumina aggregate, fused silica aggregate, graphite and binder unaltered.

(ii) To study the physical properties like apparent porosity (AP) and bulk density (BD), mechanical properties like cold modulus of rupture (CMOR), cold crushing strength (CCS), and modulus of elasticity (MOE), thermal expansion coefficient (TEC) and thermo-chemical properties like oxidation resistance and erosion resistance as a function of alumina aggregate (amount and type) and

(iii) To study the effect of metallic silicon addition on the above properties as a function of alumina aggregates type.

CHAPTER 4

Chapter-4 Experimental Details

The raw materials used for the preparation of Al_2O_3-C refractory were brown fused alumina, white fused alumina, tabular alumina, fused silica, graphite and resin. repared in this Base composition for the alumina-graphite refractory is consisting of Alumina(45 wt%),Fused silica(28 wt%) and Graphite(27 wt%) and Phenolic Resin as Binder.

4.1 Raw Materials

White fused alumina,Brown fused alumina,Tabular alumina, Fused silica, Graphite [94% fixed carbon] were used as the aggregates for Al_2O_3-C refractory. Novolac (cured by hexamethylene tetramine) and resol type phenolic resin were used as binder and Fine Si metal powder was used as additive (antioxidant). The specifications of the raw materials used in this study are given in Table 4.1.

Table 4.1 Specifications of the Raw materials used in this study

COMPOSITION (wt%)	WFA	BFA	TA	FLAKY GRAPHITE	FUSED SILICA	Si METAL POWDER
Al_2O_3	99(min)	93-94	99(min)	-----	0.1	0.1
Fe_2O_3	0.1	0.4	0.1	-----	0.1	0.7
SiO_2	----	----	-----	-----	99(min)	----
TiO_2	-----	2.6	-----	-----	-----	-----
Si	-----	-----	-----	-----	-----	97
Fixed Carbon	-----	-----	-----	94	------	-----

Specifications of the binder used:

Liquid resin- Viscosity (800 cps), 79 % fixed carbon

Powder resin- hexamine (11%), M.P-77^{0}C

Table 4.2 Specification of slag used

Al_2O_3 (%)	Fe_2O_3 (%)	MgO (%)	CaO:SiO_2
2-3	20-25	7-10	3

4.2 Sample Preparation

The batch size for Al_2O_3-C refractory was 20 kg. The requisite amounts of aggregates were mixed in a 50 Kg capacity Z-Kneader mixture machine for 5 minutes. Mixture temperature was maintained at 150^{0}C. Then powder resin was added to the mixture and dry mixed for 3 minutes. Then liquid resin was added in the mixture and mixed for 15-20 minutes in order to achieve proper consistency of the mixture. The mixture was the unloaded into a tray and kept it inside controlled humidity and temperature chamber for curing (for 24 hr). The lump formed if any after curing was crushed and screened properly. Then volatile material was checked for the mixture and was found to be 1.85%. Cylindrical rubber moulds were filled with this mix by vibro-ramming in order attain uniform filling of the material inside the mould. The mould were then cold isostatically pressed (CIP) at 1500 bar pressure. The CIP samples were dried at 240^{0}C for 16 hr. The dried samples were then fired at 1050^{0}C for 3 hr under reducing atmosphere (coke atmosphere). Samples for different testing were cut from these fired specimens. The flow sheet for the sample preparation of Al_2O_3-C refractories is as shown in the flow sheet(Fig.4.1)

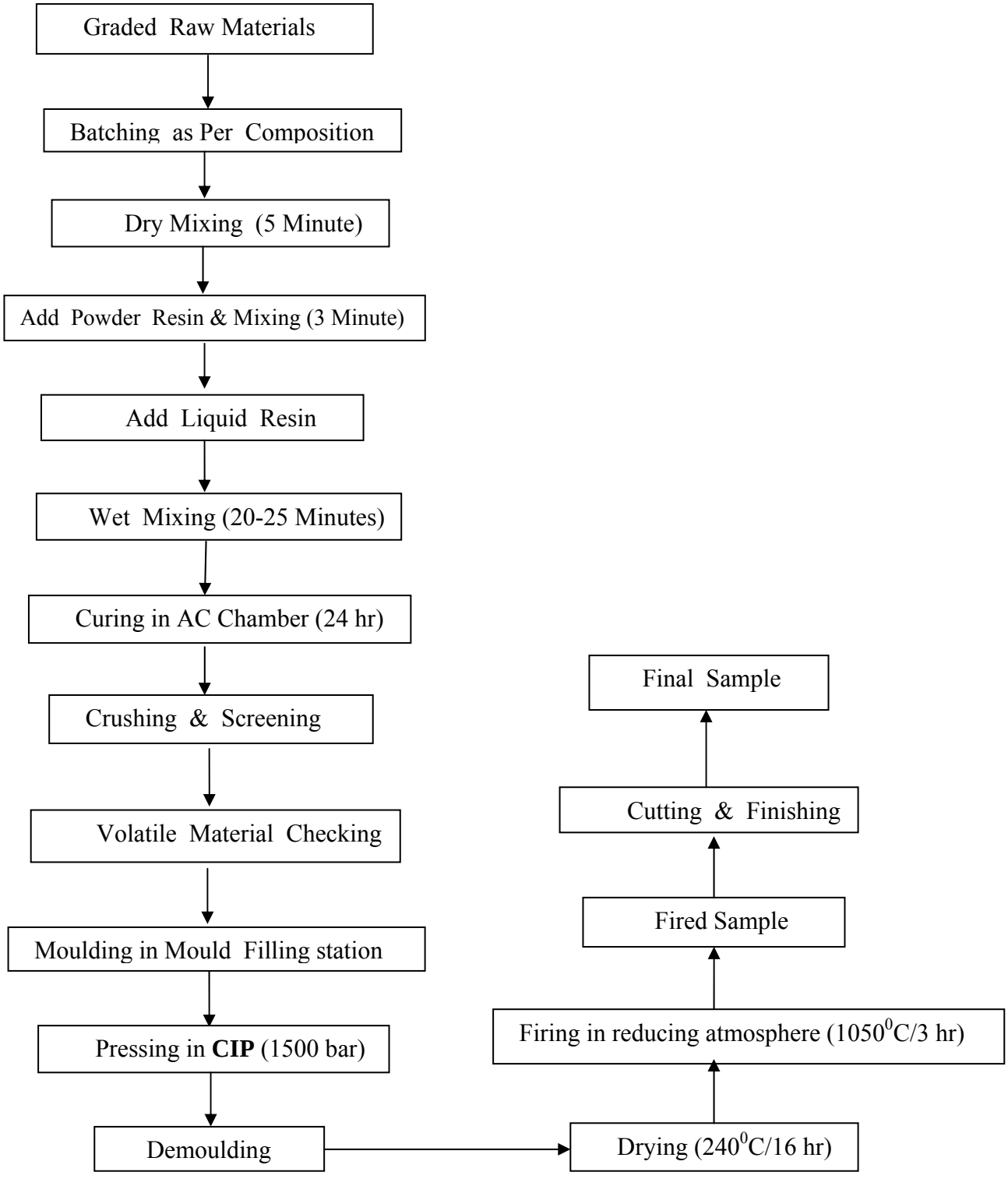

(Fig.4.1 Flow Sheet for the Preparation of Al_2O_3-C sample)

4.3 Characterization of Al_2O_3-C refractory

For the quality assurance program, the testing and evaluation of samples are carried out in accordance with the international standards or well-established procedures mutually agreed between the user and supplier of refractories.

4.3.1 Apparent Porosity and Bulk Density

Apparent porosity and bulk density of samples were determined as per ASTMC -20 as follows. Archimedean evacuation method was followed for the measurement of both bulk density and apparent porosity fired sample using water as the medium. The sample size was 30 × 40×40 mm for the measurement. The dry weight of the test samples were taken and then transferred to airtight desiccators, which was then evacuated until a minimum pressure was reached. After the vacuum was attained for 30 min, water was introduced into the desiccators. The specimens were completely covered with water to fill all the open pores. After that, the specimens were suspended in water and reweighed. Finally the soaked test piece was reweighed in air. The dry, suspended and soaked weights of the samples were taken as follows:

Dry weight of the sample = W_d gm

Suspended weight of the sample = W_{Su} gm

Soaked weight of the sample = W_{Skd} gm

Density of water = 1gm/cc

The bulk density and apparent porosity of the samples was calculated as follows:

$$\textbf{Apparent Porosity (\%)} = \frac{Wskd - Wd}{Wsku - Wsu}$$

And

$$\textbf{Bulk Density (gm/cc)} = \frac{Wd \times \text{Density of Water}}{Wsku - Wsu}$$

4.3.2 Cold Modulus of Rupture

The cold modulus of rupture of the fired samples was measured as per ASTMC – 133. This test is designed to determine the modulus of rupture (flexural strength in three-point bending) at room temperature. The instrumental apparatus used for this observation was UNIVERSAL TESTING MACHINE (TINIUS OLSEN). Modulus of rupture is the maximum stress that a

rectangular test piece of specified dimensions can withstand when it is bent in a three-point bending device. It is the ability of a bar or slab to resist failure in bending. Five samples of each batch were taken to determine the flexural strength and the average values have been reported. Flexural strength was determined by three-point bending method in an instrument. The span length of 125 mm was maintained for this measurement. Test specimen size was 150×25×25 mm. The test specimens were placed in such a way that the load applied is at middle of the span. The loading rate should be uniform during testing. Flexural strength was calculated from the following equation:-

$$\textbf{Modulus of Rupture (Mpa)} = \frac{3PL}{2bd^2}$$

Where, P = fracture load (kg)

L = Span length/ distance between the rollers (mm)

W = width of the sample (mm)

D = Thickness of the sample at the fracture plane (mm).

4.3.3 Modulus of Elasticity

The modulus of elasticity of the samples was measures as per ASTMC – 1548. This test determines the deformation (amount of strain) of the specimen under applied load (stress). The value of MOE can be determined by taking slope of stress vs strain curve, which can be found out from three point bending method as like flexural strength determination method at room temperature. The instrumental apparatus used for this observation was UNIVERSAL TESTING MECHINE(TINIOUS OLSEN).In this case five samples, each having dimension of 150×25×25mm was tested. The span length was 125 mm. Then MOE value for each sample has been calculated from the slope of the stress vs strain curve and finally average of the five values was taken for consideration.

$$\textbf{Modulus of Elasticity (MPa)} = \frac{STRESS}{STRAIN}$$

4.3.4 Cold Crushing Strength

Cold crushing strength of the refractory specimens was measured as per ASTMC – 133. Cold crushing strength of the refractories has been measured by placing a suitable refractory specimen on flat surface followed by application of uniform load to it through a bearing block in a standard mechanical or hydraulic compression testing machine. The load at which crack appears the refractory specimen represents the cold crushing strength of specimen. The load is applied on the sample in the flat position (Fig 4.2). The centre of the spherical bearing block is in contact with the top bearing surface of the specimen and is in the vertical axis of the specimen. The load is applied uniformly during the test. Four samples of each batch were taken to measure the compressive strength and the average values have been reported. Test specimen size was 25×25×25 mm. The working formula for calculating CCS is given by,

$$\textbf{Cold Crushing Strength (Mpa)} = \frac{W}{A}$$

Where, W = Total maximum load in kg, and

A = Average of the gross areas of top and bottom in mm^2.

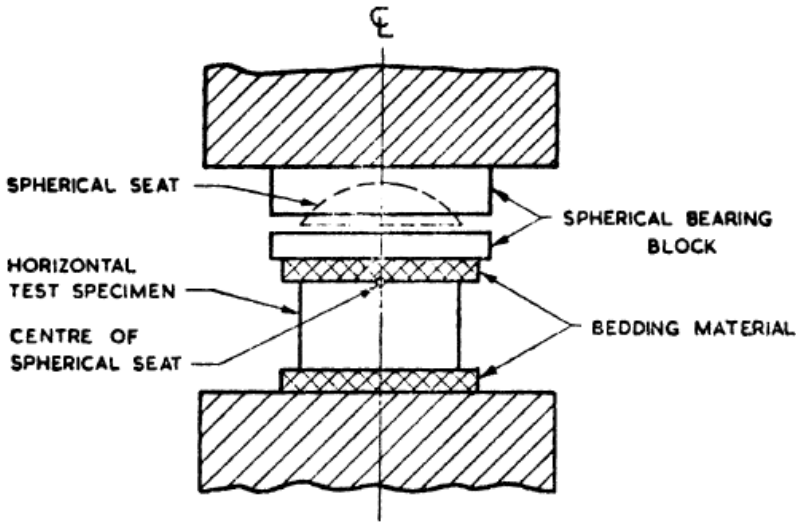

(Fig.4.2 A Sample for Cold Crushing Strength Testing)

4.3.5 Thermal Expansion Coefficient

This method determines the thermal expansion co-efficient (α) value for the sample in the temperature range room temperature to 1000^0C. In this case, the samples were cut into small rectangular pieces about 20 mm length. The change of length of the sample was measured under an inert atmosphere (Argon gas). Prior to the testing, argon gas was put inside the dilatometer (NETZSCH DL 402C) for creation of an inert atmosphere. The heating rate was maintained at 10^0C/min. Finally the thermal expansion coefficient value for the given sample was calculated from the graph. The testing was correlated to ASTMC-832.

4.3.6 Thermal Spalling Resistance

The standard method of finding out spalling resistance is heating the material at an elevated temperature followed by sudden cooling in air at ambient temperature. The quantification was done by the number of cycles to withstand such temperature fluctuations. Prior to the testing of the samples, they were coated with high temperature coating materials. 0The sample specimen of 30×40×40mm were heated at 1200ºC and then suddenly brought down to ambient condition by cooling it in air for 10 minutes. The number of cycles the specimen resists was noted down as the spalling resistance. The testing was correlated to ASTMC-1171.

4.3.7 Oxidation Resistance

This method determines the oxidation thickness of the sample when subjected to high temperature in air. Three samples from each batch were taken, each having dimension of 30×40×40mm.Then the samples were placed inside the furnace for testing at different temperatures i.e. 800^0C and 1200^0C for 2 hours of soaking periods. After cooling, the oxidized samples were taken out from the furnace and finally their oxidation thicknesses were measured by slide calipers.

4.3.8 Erosion Resistance

Erosion resistance of the samples was observed by rotary slag test in rotary drum instrument. In this case one sample (dimension 160×30×40mm) from each batch was taken. The samples were then coated with high temperature coating material followed by drying inside dryer for 1 hour. Then about 10 samples were lined inside the sample holder by using mortar for setting purpose. Then after drying (in room temperature) the drum was fitted to the rotary drum machine. Prior to the start of testing, the apparatus was connected to gas cylinders and the pressure of gas was checked properly. Then the rotating speed of the rotary drum was maintained at 5 rotations per minute. Before the start of testing with slag and metal, the samples were preheated at 1000^0C for 1 hour. Then about 250 gm of metal (iron rod) was added through the orifice of the sample holder. After 30 minutes 250gm of LD slag was put inside the sample holder. Simultaneously the temperature was increased to 1550^0C by increasing the gas pressure and fuel supply. The temperature was kept constant at 1550^0C for 1 hour. The temperature of testing was observed by means of pyrometer. After 30 minutes of testing, the molten metal and slag was tapped out from the machine and fresh slag and metal again added to it for further testing. Similarly, another tapping was done after 30 minutes. After 2 nos. of tapping, the test was stopped and after cooling the eroded samples was taken out of the rotary drum and the eroded depth was measured by means of slide calipers. The testing was done on the basis of ASTMC-874.

4.3.9 Particle Size Analysis

In order to find out the particles size distribution, the alumina powder was dispersed in water by ultrasonic processor [Oscar Ultrasonic].Then experiment was carried out in computer controlled particle size analyzer MALVERN MASTER SIZER (UK).The dispersant used in this case was sodium hexametaphosphate. The particle diameters vs. cumulative volume % graphs for different raw materials were drawn by the software.

4.3.9.1 Sample Preparation for X-Ray Analysis

Prior to XRD analysis the samples that were fired at a temperature about 1000^0C and corroded samples (testing at 1550^0C/1 hr) were broken into pieces. These pieces were ground into fine powder using X-ray Diffractometer (Philips PANalytical, Netherland) machine. The X-ray analysis was carried out on these powdered samples.

4.3.9.2 Phase Analysis

The different crystalline phases in the prepared mix were determined by the XRD study. The samples were scanned at 0.04^0/min at the following instrument parameter settings:

Voltage/Current – 35kV/25mA

Incident beam slit – 0.25 mm

Divergence beam slit – 0.5 mm

Radiation - Cu-Kα, λ = 1.54056Å

Filter – Nickel

Scan Angle 2θ – $20\text{-}70^0$

Scan Speed - 0.04^0 per min

The obtained diffraction patterns were smoothened, fitted and analyzed using Philips X-pert high-score software.

CHAPTER 5

Chapter 5 *Results and Discussions*

The aggregates of alumina-carbon refractories were brown fused alumina (BFA), white fused alumina (WFA), tabular alumina (TA), fused silica and carbon. These aggregates were bonded using resin as the binder. The present investigation deals with the effect of starting alumina aggregates on the properties of alumina carbon refractories on the basis of without any metallic addition. Details study on the performance of Al_2O_3-C refractories is given as below:-

5.1 Apparent Porosity

The variation of apparent porosity (A.P) with respect to different alumina aggregates are shown in Fig. 5.1-5.3. Figure 5.1 represents the variation of AP as function of substitution of brown fused alumina (BFA) by white fused alumina (WFA) in the aggregate. It clearly shows that the substitution of BFA with WFA leads to an increase in porosity. The porosity was found to increase almost linearly with WFA substituent. Samples prepared with 100% BFA have 11.7% AP on the other hand that prepared with 100% WFA has 13.9% AP. The variation of AP was found be very small. Figure 5.2 shows the variation of AP as function of substitution of TA by BFA in the aggregate. It was found that the porosity decreases with BFA substitution up to 60% and then it increases and remains constant. Samples prepared with 100% TA have (13.2%) AP on the other hand that prepared with 100% BFA has 11.8% AP. The Minimum AP was found to be (10.6%) at 60% BFA substitution. Figure 5.3 shows the variation of AP as function of substitution of WFA by TA in the aggregate. Although the AP variation follows a regular trend for the above two substitutions, the substitution of WFA by TA does not show any definite trend.

Al_2O_3-C refractory uses resin as binder to bind the refractory aggregates. The resin binder has the disadvantage of forming open pore when fired at 1000^0C for 3 hr in coke atmosphere [4]. This is due to the burning out of volatile matters from the resin. The samples prepared in the present investigation contain same amount of resin and were fired at the same temperature. Thus the effect of resin on the AP of the samples as a function of alumina aggregates will have same contribution for all the cases. Hence the variations of AP observed in fig. 5.1-5.3 are not due to the resin content but for the variation of the aggregates only. The particle size distribution for

different alumina aggregates used in this study has been provided in Fig. 5.4. The BFA and WFA aggregates shows monomodal distribution whereas TA aggregates follows a bimodal distribution. The particle size distribution shows that the BFA aggregates have a narrow particle size distribution as compared with WFA. The average particle sizes for the aggregates were 45μm, 47μm and 52μm respectively for BFA, WFA and TA. The population of more volume fraction of smaller particles in case of BFA is responsible for low AP in the samples prepared with 100% BFA as compared with 100% WFA samples. The almost linear increase in AP as observed in Fig.1 could easily be explained from the additive nature of the AP. BFA has a slightly lower particle size than TA, thus incorporation of BFA to TA causes an decrease in AP due to the filling of the inter-particle porosity of TA aggregates by BFA as observed in Fig. 4.2. The unusual irregular trend as observed in Fig. 3 may be due to the bimodal distribution of the TA aggregates.

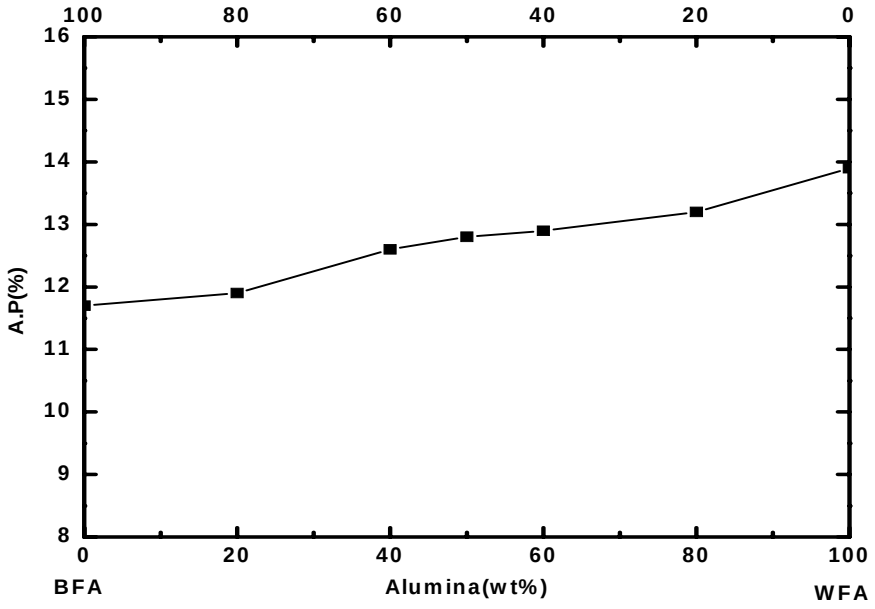

Fig.5.1 variation of Apparent Porosity for samples containing WFA and BFA

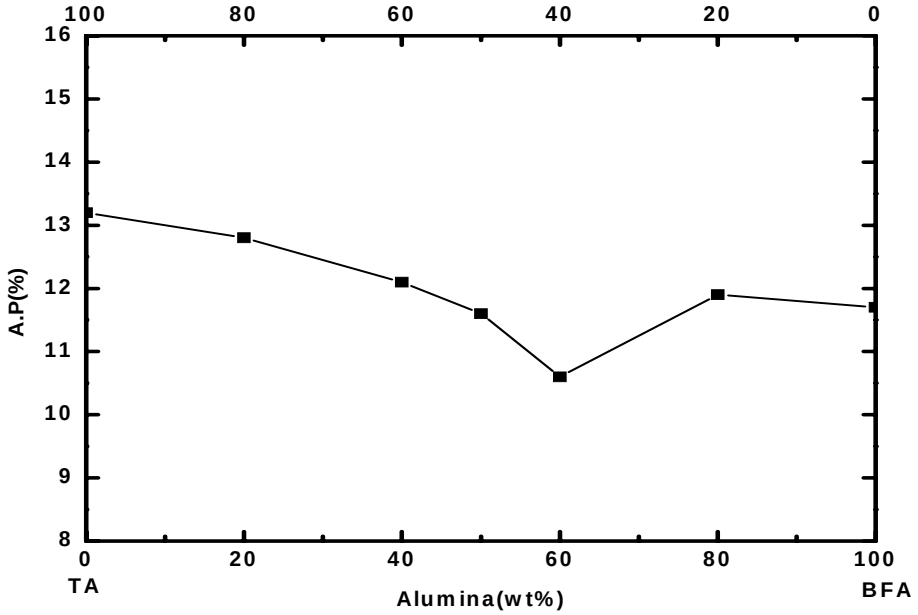

Fig.5.2 Variation of Apparent Porosity for samples containing BFA and TA

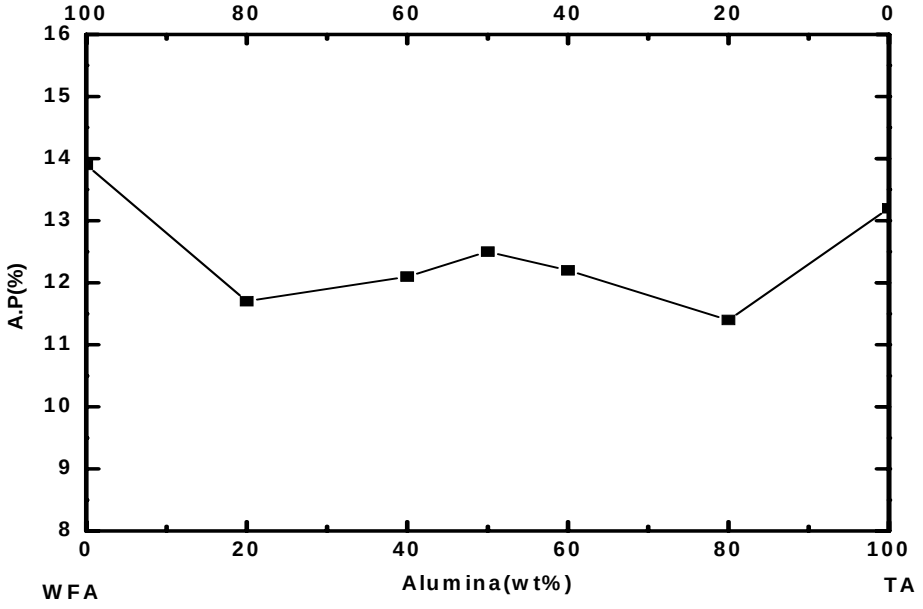

Fig.5.3 Variation Apparent Porosity for samples containing TA and WFA

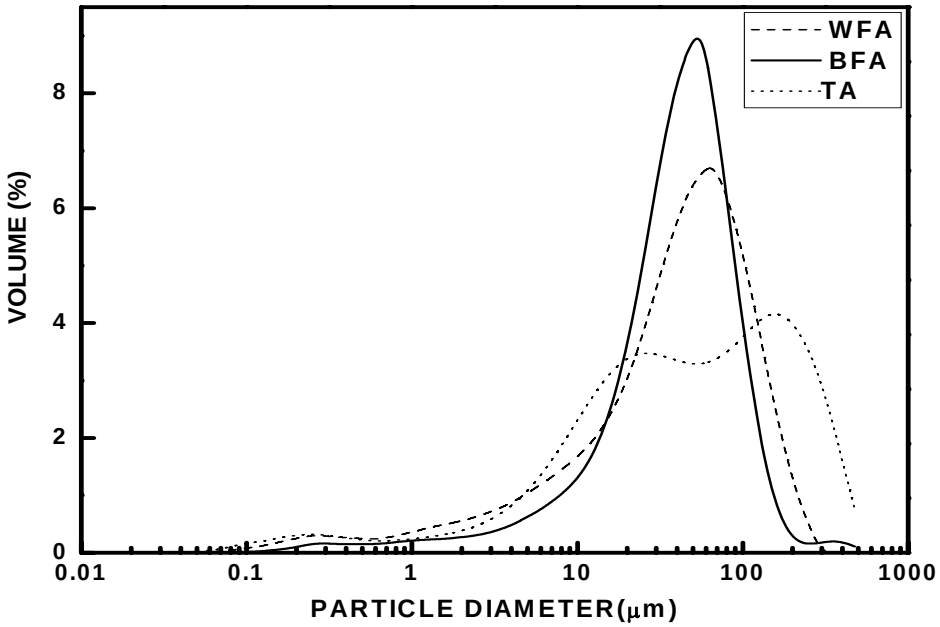

(Fig.5.4 Particle size distribution of different alumina aggregates)

5.2 Bulk Density

The bulk density (B.D) variation for different alumina aggregates are shown in Fig. 5.5-5.7. Figure 5.5 shows that the B.D decreases for the samples when the substitution of BFA was made by WFA. Although the variation is very small the BD of the samples were found to follow almost a linear variation. This variation could be explained easily from the particle size distribution of the aggregates as discussed earlier (Fig.5.4). The variation of BD in the samples due to incorporation of BFA in TA is shown in Fig.5.6. It has been found that the BD increase with BFA substitution initially and then decreases. The initial increase in BD is due to the accommodation of finer BFA aggregates in to the inter-particle voids of the TA particles. Figure 5.7 represents the variation of BD in the samples upon replacement of WFA aggregates by TA. The variation of BD in the samples follows the reverse trend as observed in case of AP when WFA is substituted by TA aggregates, which is very much obvious.

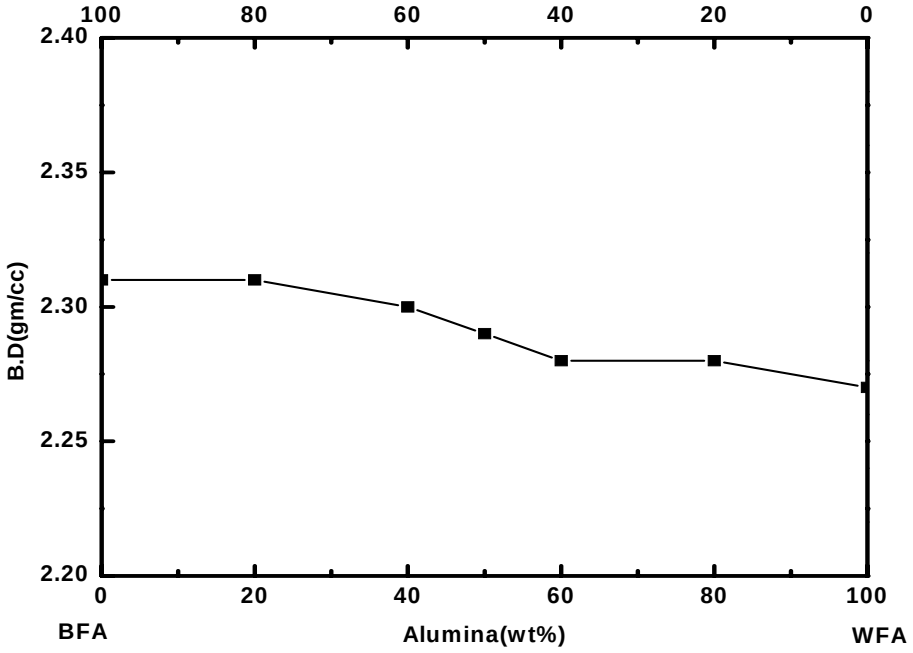

Fig.5.5 Variation of Bulk density for sample containing WFA and BFA

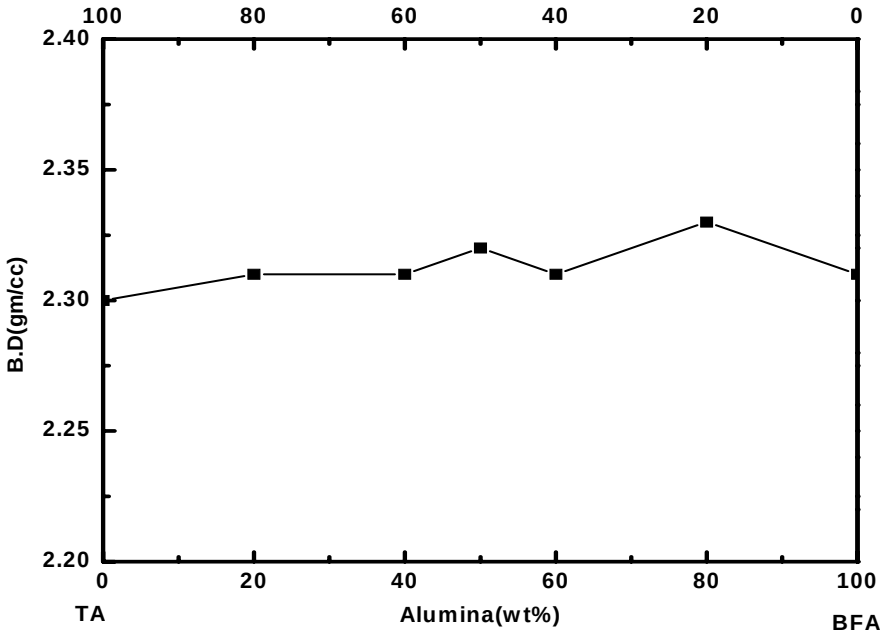

Fig.5.6 Variation of Bulk density for sample containing BFA and TA

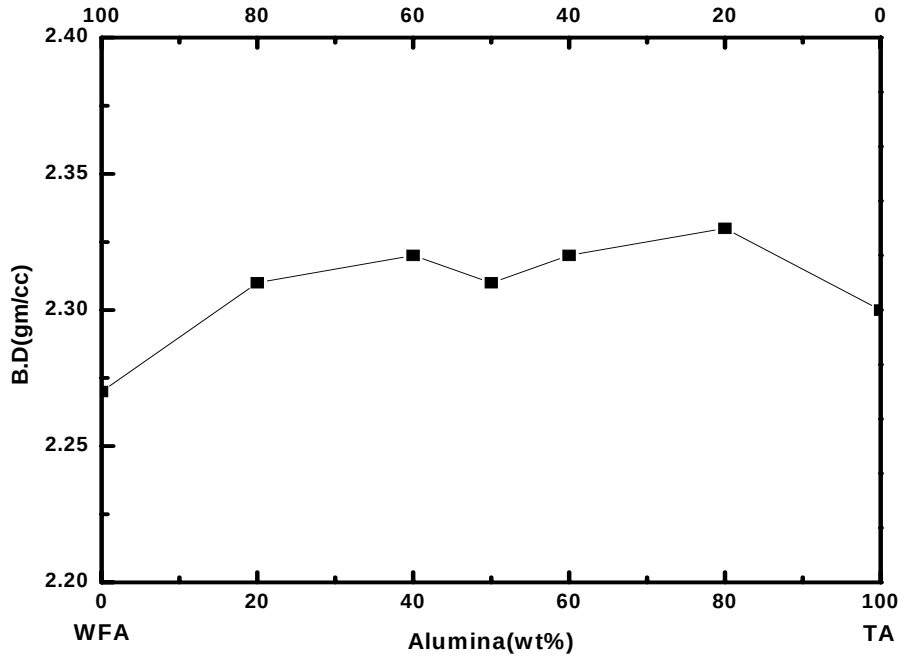

Fig.5.7 Variation of Bulk density for sample containing TA and WFA

5.3 Cold Modulus of Rupture

The flexural strength (or modulus of rupture) of a material depends on grain size, grain shape, phase assembly, nature and amount of vitreous phase present in the raw materials used during processing [40]. Binder used for the alumina carbon refractory is resin, which binds all the refractory aggregates together and produces plasticity during subsequent curing. Hence the types of resin bonding may be a factor that is responsible for the modulus of rupture. The apparent porosity plays an important role in the MOR variation with respect to different alumina aggregates. The variations of modulus of rupture (MOR) for different aggregate substitutions were shown in the Fig. (5.8 - 5.10).

Figure 5.8 shows the variation of MOR as BFA aggregates are substituted with WFA. It shows that that there is a sudden increase in MOR value observed at 20% WFA incorporation in BFA there after it decreases gradually up to 100% substitution. The gradual decrease in MOR can be explained by means of individual grain strength of the aggregates. WFA aggregates have lower

strength than that of BFA. Hence MOR decreased with increase in WFA substitution. The variation of MOR as a function of BFA substitution to TA is shown in Fig. 5.9. In this substitution it has been observed that there is a sudden jump in MOR value at 20% BFA substitution thereafter it decreases gradually up to 100% substitution. The decrease in MOR value with increase in WFA substation can be explained easily from the surface morphology of the aggregates used. The surfaces of BFA grains are smooth as compared with the TA grains due to the porous structure of TA [4]. Thus BFA aggregates attain a weaker bonding with the resin as compared with TA. Hence, the decrease in MOR value on BFA substitution to TA is attributed to the bonding of the aggregates with the resin. Figure 5.10 shows the variation of MOR as a function of TA replacement in WFA aggregates. It has been observed that the MOR value increases gradually up to 80% replacement of WFA by TA, thereafter it decreases suddenly. The gradual increase in MOR value with increase in TA substitution may be explained as follows. The rough surface with shallow semispherical pores of TA aggregates enhances mechanical interlocking with the bonding matrix and provides high bending strength [5].

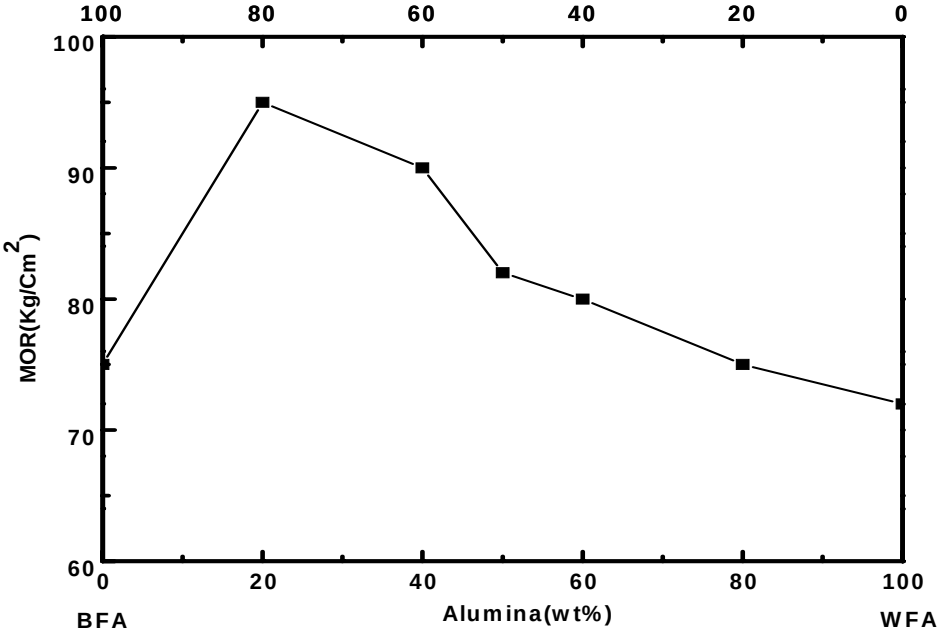

.

Fig.5.8 Variation of MOR for sample containing WFA and BFA

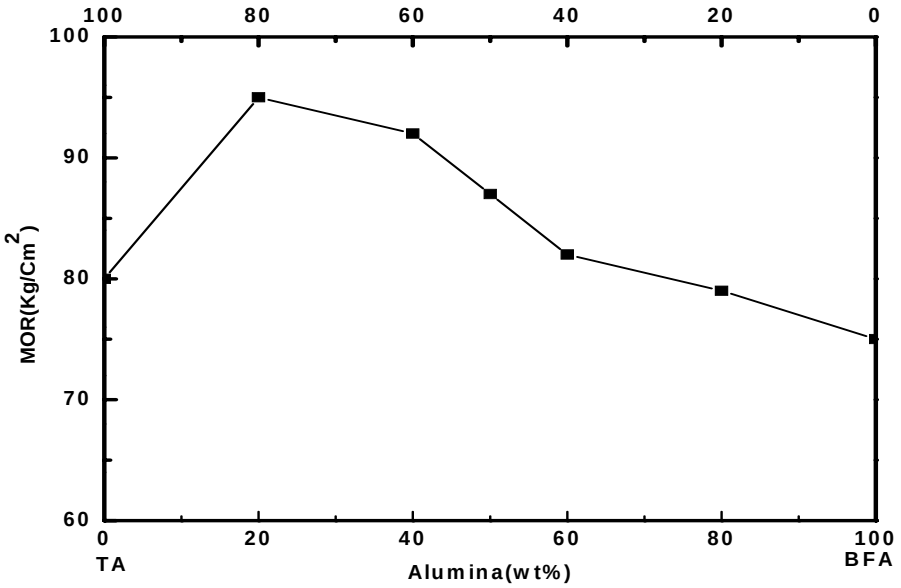

Fig.5.9 Variation of MOR for sample containing BFA and TA

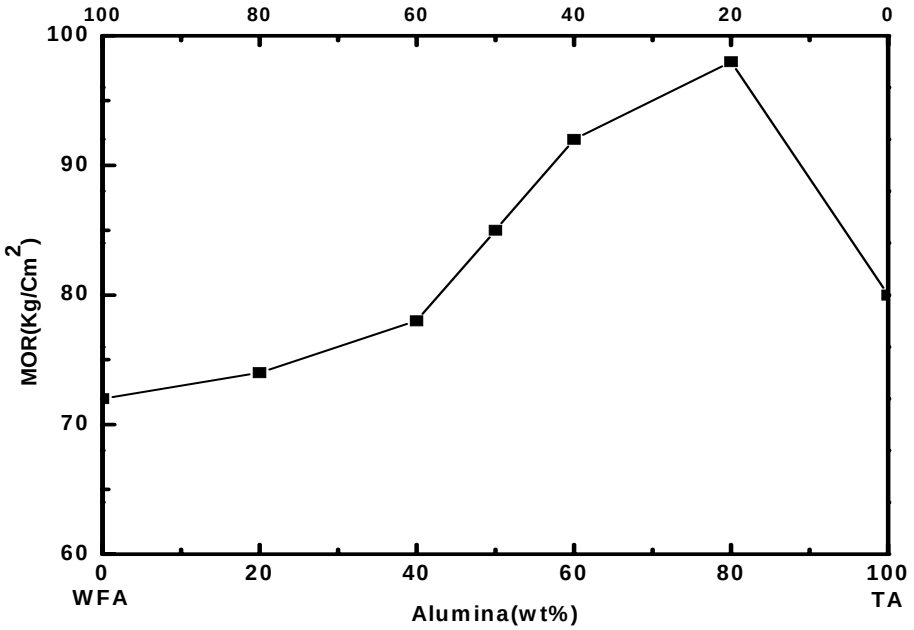

Fig.5.10 Variation of MOR for sample containing TA and WFA

5.4 Cold Crushing Strength

The variations of cold crushing strength (CCS) for different aggregate substitutions were shown in the Fig. (5.11-5.13).

Figure 5.11 shows the variation of CCS as BFA aggregates are substituted with WFA. It could be seen that there is a sudden increase in CCS value at 20% WFA incorporation in BFA there after it decreases gradually up to 100% substitution. The gradual decrease in CCS can be explained by means of individual grain strength of the aggregates. WFA aggregates have lower strength as compared to that of BFA .hence CCS decreases with increase in WFA substitution. The variation of CCS as a function of BFA substitution to TA is shown in Fig.5.12. In this substitution it has been observed that there is also a sudden jump in CCS value at 20% BFA substitution thereafter it gradually decreases up to 100% substitution. The decrease in CCS value with increase in WFA substation can be explained easily from the surface morphology of the aggregates used. The surfaces of BFA grains are smooth as compared with the TA grains due to the porous structure of TA aggregates. Thus BFA aggregates attain a weaker bonding with the resin as compared with TA. Hence, the decrease in CCS value on BFA substitution to TA is attributed to the bonding of the aggregates with the resin. Figure 5.13 shows the variation of CCS as a function of TA replacement in WFA aggregates. It has been observed that the CCS value increases gradually up to 80% replacement of WFA by TA, thereafter it decreases suddenly. The gradual increase in CCS value with increase in TA substitution may be explained as follows. The rough surface with shallow semispherical pores of TA aggregates enhances mechanical interlocking with the bonding matrix and provides high compressive strength [5].

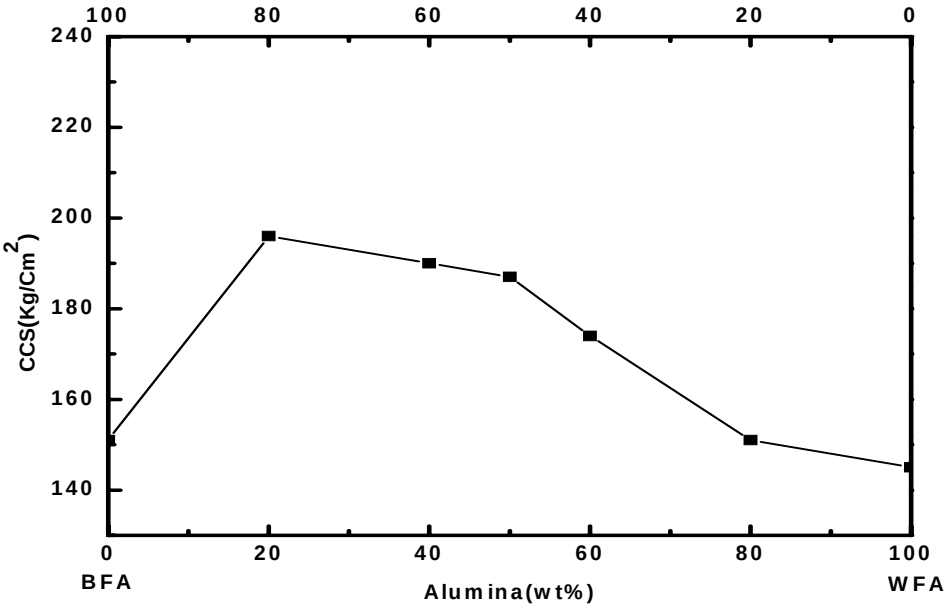

Fig.5.11 Variation of CCS for sample containing WFA and BFA

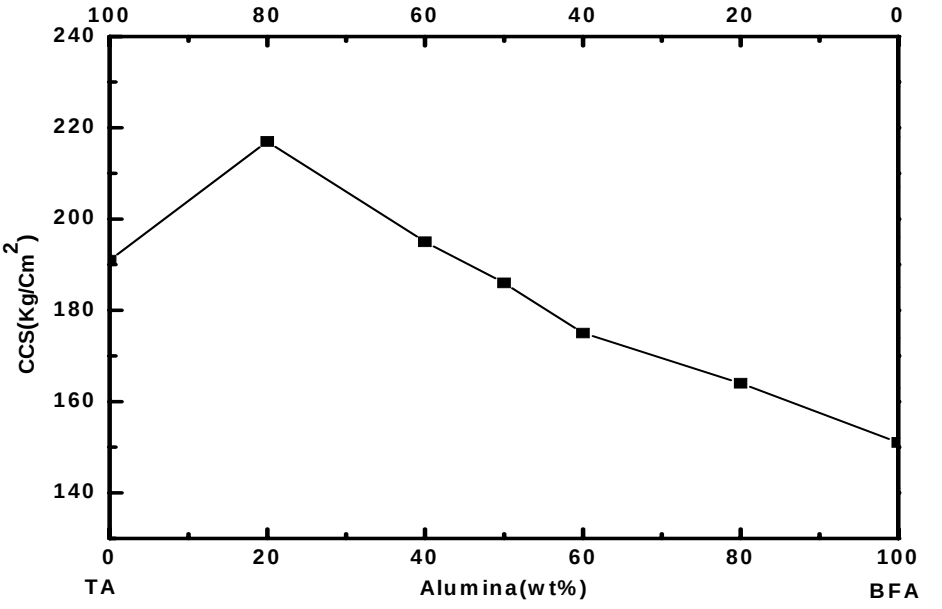

Fig.5.12 Variation of CCS for sample containing BFA and TA

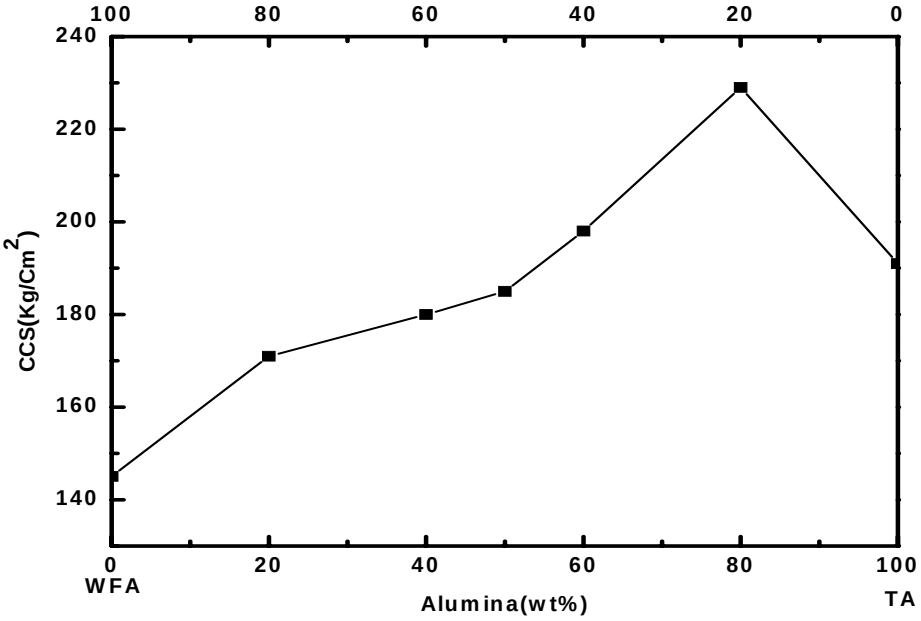

Fig.5.13 Variation of CCS for sample containing TA and WFA

5.5 Modulus of Elasticity

The variation of modulus of elasticity (MOE) as a function of different alumina aggregates are presented in Fig.5.14-5.16. MOE of a material depends on the volume fraction of porosity of a material the lower the porosity MOE will be low. MOE of refractory material was found to be dependent on the type of aggregates used mainly the grain size, shape or in the other wards the grain morphology of the aggregates. Figure 5.14 shows the variation of MOE of alumina – carbon refractories when BFA aggregates were replaced with WFA. It clearly shows that there is a sudden decrease in MOE value for 20% WFA replacement in BFA thereafter it increases gradually. The gradual increase in MOE value with increase in WFA substitution may be due to the softness of the WFA aggregates as compared with BFA. The variation of MOE as a function of BFA substitution to TA is shown in Fig.5.15. It has been found that the MOE gradually decreases up to 80% BFA substitution then it suddenly increases. The gradual decrease in MOE value with BFA substitution to TA can be easily explained from the aggregate morphology. The TA aggregates have more irregular, rough surface as compared to BFA [4]. The rough TA

surface provides better bonding with the resin bond as responsible for providing high MOE value in the sample. Figure 5.16 shows the variation of MOE as WFA in the alumina carbon refractory is replaced by TA aggregates. It could be seen that there is a sudden decrease in MOE on 20% TA replacement to WFA thereafter it increases gradually up to 100% substitution. The gradual increase in MOE is due the rough surface of the TA aggregates as compared to WFA. This rough irregular surface provides better bonding with the resin and attributed to the gradual increase in MOE value of the sample.

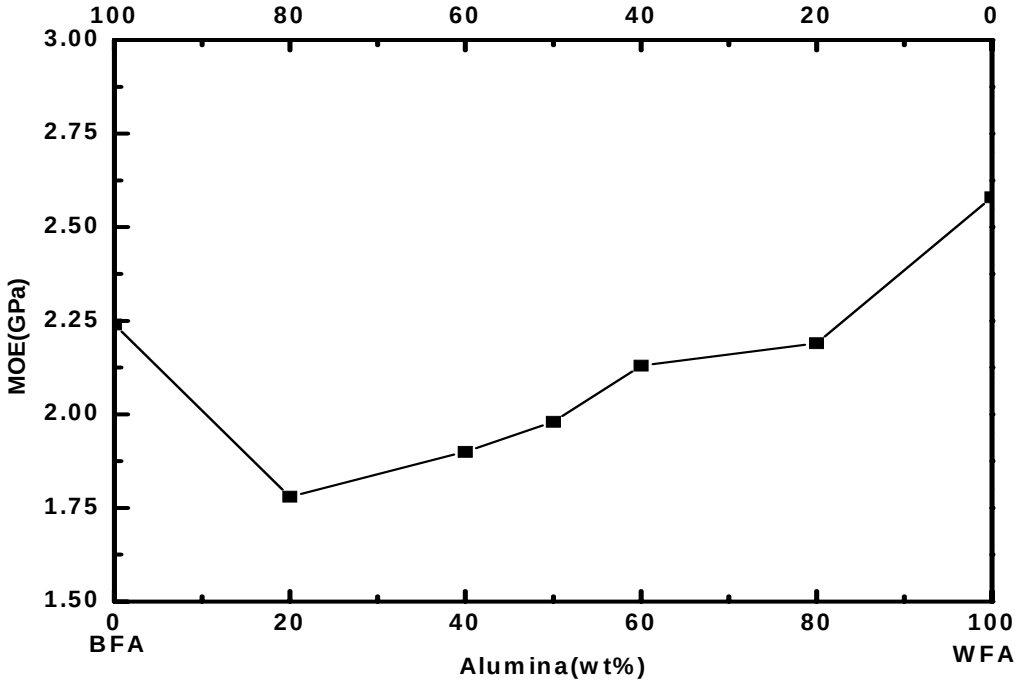

Fig.5.14 Variation of MOE for sample containing WFA and BFA

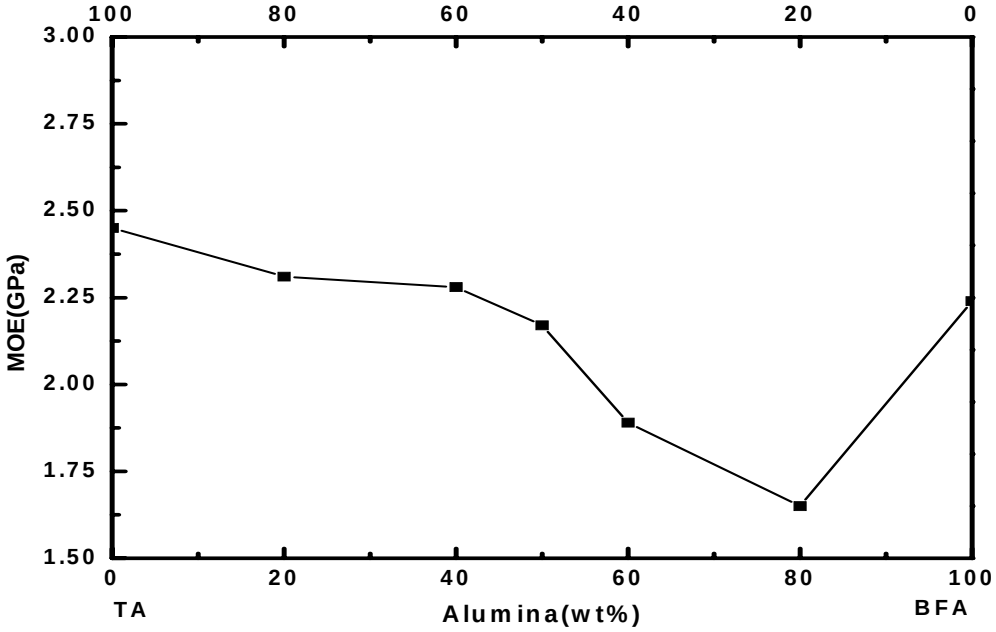

Fig.5.15 Variation of MOE for sample containing BFA and TA

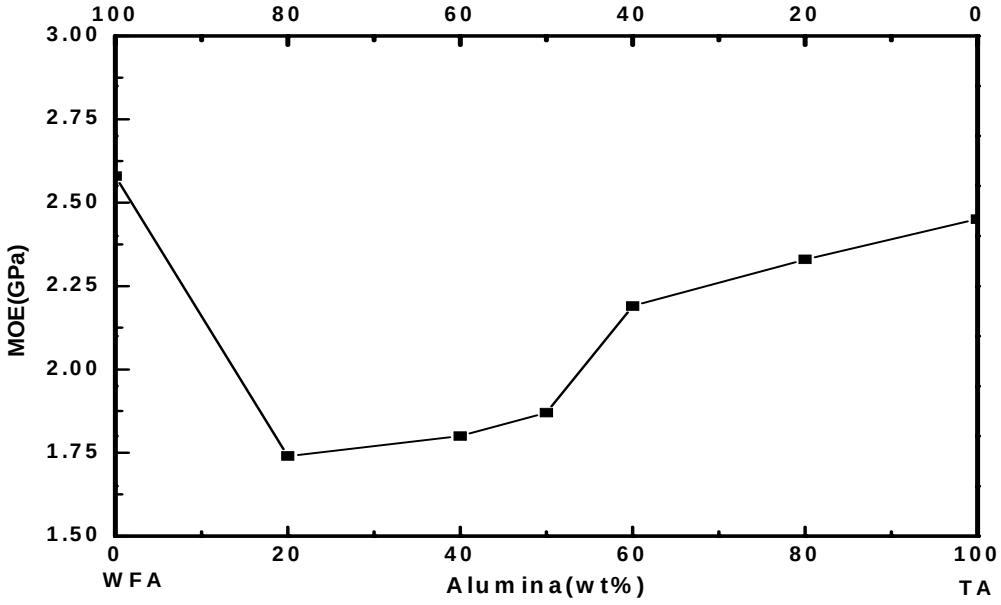

Fig.5.16 Variation of MOE for sample containing TA and WFA

5.6 Thermal Expansion

Thermal expansion coefficient (TEC) is an additive property and thus for refractory depends on the expansion coefficients of the individual components. The variation of thermal expansion coefficients of alumina carbon refractory as a function of different alumina aggregates are presented in Fig. 5.17-5.19. The thermal expansion coefficient variations as shown in Fig. 5.17-5.19 are due the variations of the alumina aggregates only as the other components remains constant in the present study. Figure 5.17 shows the variation of TEC as a function of WFA substitution to BFA. It could be seen that the thermal expansion gradually decreases with increase in WFA replacement to BFA. This is due to the higher TEC value of BFA (α=8.52) as compared to WFA (α=8). The higher TEC value of BFA is due the inherent iron and titania content in BFA. The variation of TEC on TA replacement by BFA is shown in Fig. 5.18. The TEC value was found to increase with the increase in BFA substitution in this case although the variation is very small. TA (α=7.58) has lower TEC value than that of BFA. Thus the gradual increase is quite obvious. Figure 5.19 shows the variation of TEC as a function of TA substitution to WFA. It has been found that the TEC value increases initially up to 20% TA replacement and then decreases up to 80% substation and thereafter it again increases. The decrease in TEC value with increase in TA substitution could easily be explained from the additive nature of the TEC.

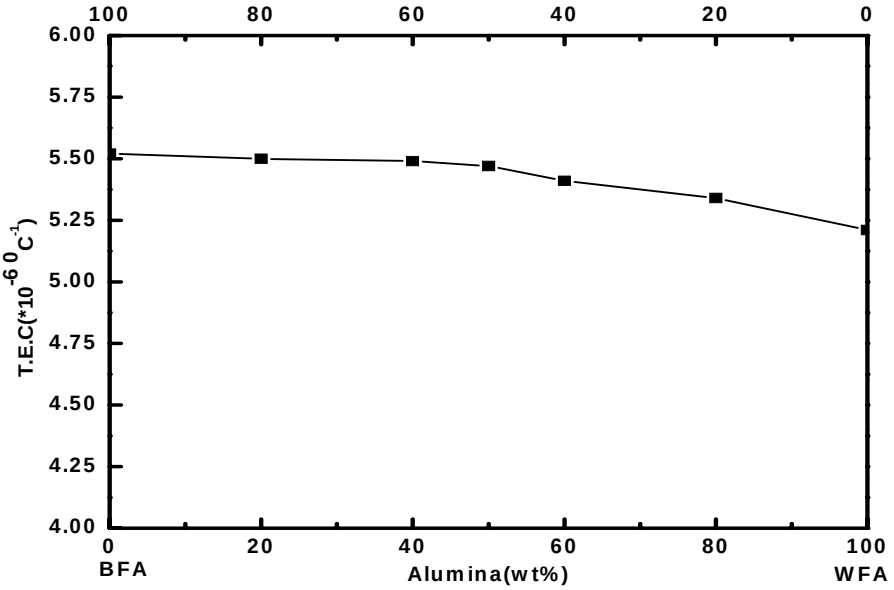

Fig.5.17 Variation of TEC for sample containing WFA and BFA

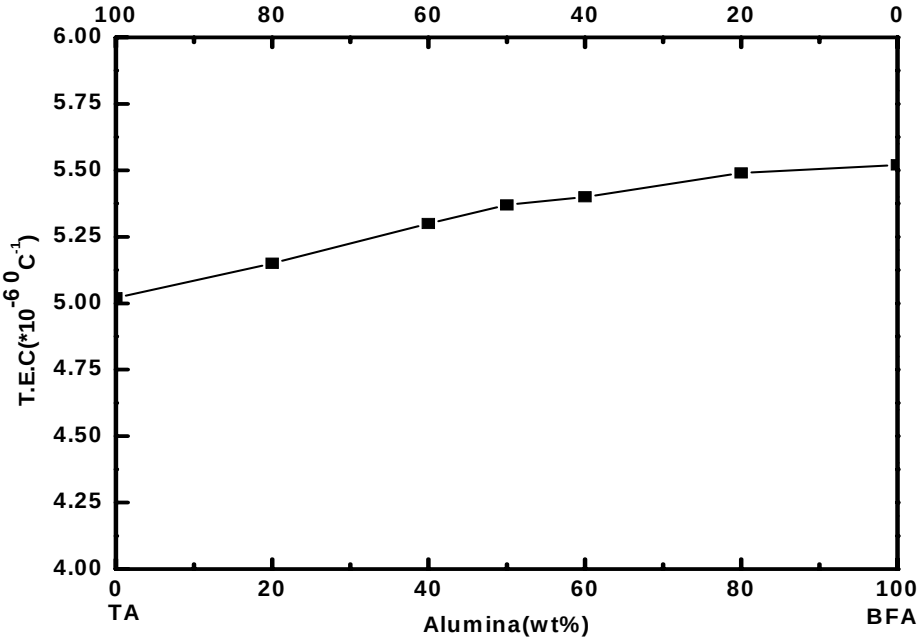

Fig.5.18 Variation of TEC for sample containing BFA and TA

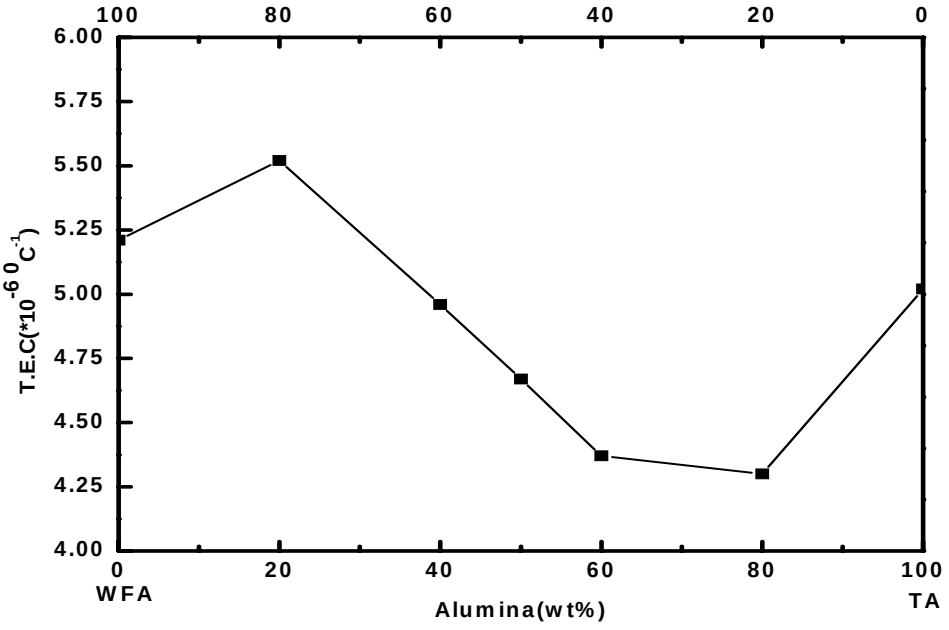

Fig.5.19 Variation of TEC for sample containing TA and WFA

5.7 Oxidation Resistance

Oxidation of carbon-carbon bond depends on the texture i.e grain size distribution and purity of raw materials used. It also depends on the porosity and pore size distribution. The oxidation layer thickness was found to increase with increase in temperature of testing. It has been reported that Al^{+3} in alumina acts as an electron acceptor against C^4 and weaken C-C bond and hence alumina accelerates the oxidation of graphite greatly. On the other hand, TiO_2 and MgO inhibit the oxidation as TiO_2 donates electrons to graphite and stabilise its structure [38]. High porosity resulted in carbon containing samples due to irreversible expansion of graphite at high temperature may also affect the oxidation resistance. All the carbon containing refractories were preheated at 1000^0C for 3 hr in a coke bed to remove volatile species before oxidation test. This heat treatment leads to the organic matters burnout present in the samples and results in open porosity generation in the materials and hence enhances oxidation phenomena [38].

Carbon, in Al_2O_3-C refractories, is oxidized in two ways (i) direct oxidation and (ii) indirect oxidation [29]. Direct oxidation occurs according to Eqn. (1) under 1400^0C, when carbon is

oxidized directly by the oxygen from atmosphere. Indirect oxidation occurs following Eqn. (2) above 1200^0C where carbon is oxidized by the oxygen from Al_2O_3.

$$\mathbf{2C(s) + O_2(g) \longrightarrow 2CO(g)} \qquad \text{----------(1)}$$

$$\mathbf{C(s) + Al_2O_3(s) \longrightarrow Al(g) + CO(g)} \qquad \text{----------(2)}$$

In early stage of oxidation, the overall oxidation rate is controlled by the chemical reaction rate on the surface of sample. As the oxidation proceeds, a porous oxidized layer gradually forms near the surface and the reaction interface moves inward. In this condition, gaseous oxygen must diffuse through this layer to reach reaction interface and hence the oxidation rate decreases. The oxidation rate was found to increase with oxidation temperature due to increase chemical reaction rate and effective diffusion rate [39].

The oxidation thickness variation as a function of different alumina aggregates has been presented in Fig. 5.20-5.22. Figure 5.20 shows the variation of oxidation thickness on replacement of BFA with WFA. The oxidation thickness was found to increase gradually with increase in WFA substitution. This is due to the presence of open pores and higher volume fraction of micropores in the WFA as compared with BFA. Oxygen from the atmosphere penetrates through these pores and oxidized the carbon present in the refractory sample. The variation of oxidation thickness as a function of TA substitution with BFA is shown in Fig.5.21. It could be found that there is sudden increase in oxidation layer thickness up to 20% BFA substitution thereafter it decreases gradually with BFA substitution. The BFA aggregates are more impervious than that of TA aggregates due to the presence of a glassy phase on the BFA aggregates. This limits the oxygen penetration through the BFA as compared with TA aggregates. Thus the oxidation layer thickness decreases with increase in BFA substitution. Figure 5.22 shows the variation of oxidation layer thickness as function of TA substitution to WFA. It has been observed that the TA substitution to WFA cause a gradual decrease in oxidation layer thickness. The gradual decrease in oxidation layer thickness may be correlated with the open porosity present within the aggregates. WFA aggregates have more open porosity as compared with that of TA, which provides the path for oxygen transport for oxidation. Hence the oxidation layer thickness was found higher in the WFA enriched samples. In all the three substitutions it has been observed that the oxidation layer thickness increases with increase in test temperature. The increase in oxidation layer thickness with increase in test temperature is due to the increase in Chemical reaction rate as well as effective diffusion rate of oxygen.

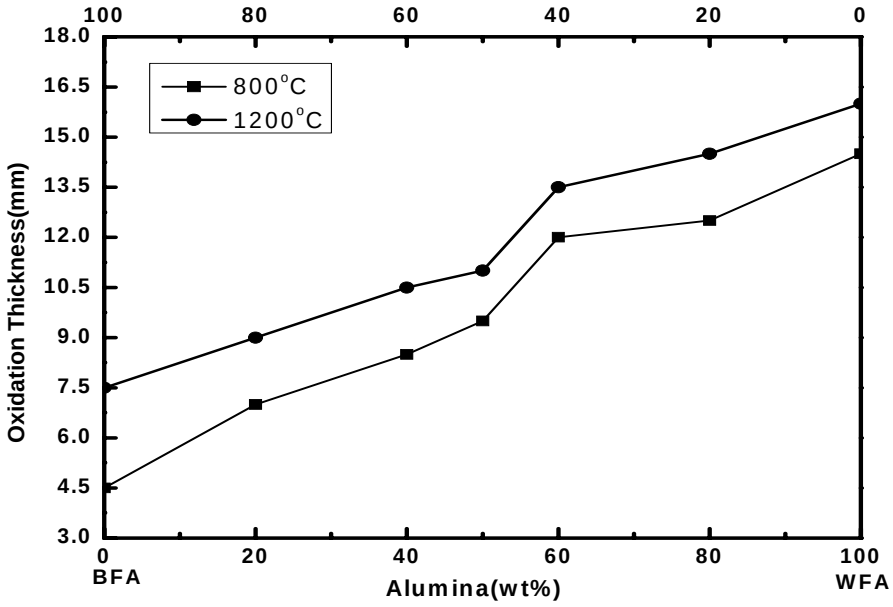

Fig. 5.20 Variation of Oxidation thickness for sample containing WFA and BFA heat treated for 2 hr of soaking period

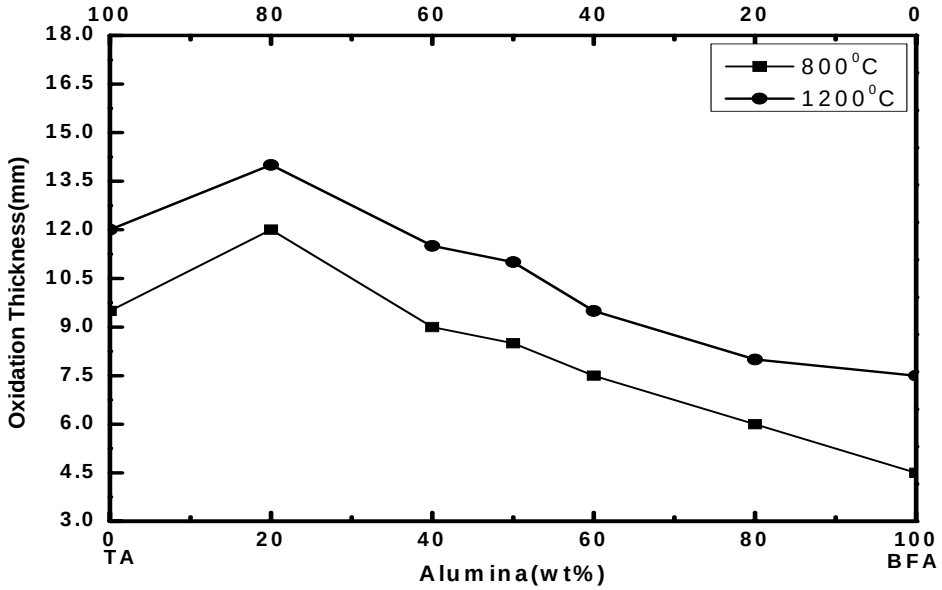

Fig.5.21 Variation of Oxidation thickness for sample containing BFA and TA heat treated for 2 hr of soaking period

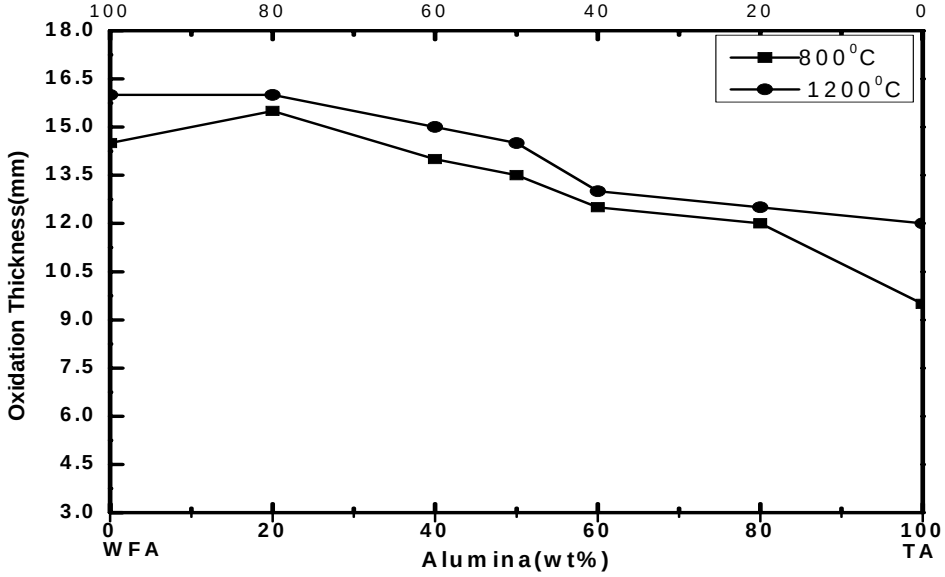

Fig.5.22 Variation of Oxidation thickness for sample containing TA and WFA heat treated for 2 hr of soaking period

Different oxidized Al_2O_3-C samples after heat treatment at 800^0C and 1200^0C were shown in the figure(5.23-5.24)

Fig.5.23 Oxidised Al_2O_3-C Samples after firing at 800^0C for soaking periods of 2 hr

Symbolic representation-W(White fused alumina),B(Brown fused alumina),T(Tabular alumina)

Fig.5.24 Oxidised Al_2O_3-C samples after firing at 1200^0C for soaking period of 2 hr

5.8 Erosion Resistance

Erosion in Al_2O_3-C refractories may be due to dissolution of alumina by slag, oxidation of carbon by iron oxide in the liquid slag, oxidation of carbon by ambient gas or direct wear by liquid iron flow [21]. It also depends on temperature and time of testing, wettability of the refractory with the slag ,quality and chemistry of materials used . High purity or fine textured raw material may reduce erosion subsequently [40]. Thermal expansion mismatch of the different components present in composite refractories leads to the development of thermal stress in the microstructure. This thermal stresses in the microstructure generates crack propagation and as a consequence, the wear of the refractory takes place by structural spalling. The continuous interaction between the slag and the refractory leads to the loss of two main refractory components, C and Al_2O_3. The Al_2O_3 loss takes place by the chemical reaction between the slag and Al_2O_3 of the refractory. On the other hand the C loss is mainly due to its oxidation by the O_2 from the atmosphere and/ or by the oxidising components such as Fe_2O_3 from the slag, which can be indicated by the following reactions.

$$2C(s) + O_2(g) \longrightarrow 2CO(g) \quad \text{----------(4)}$$

$$C(s) + O_2(g) \longrightarrow CO_2(g) \quad \text{----------(5)}$$

$$C(s) + Fe_2O_3(l) \longrightarrow 2Fe(g,l) + CO(g) \quad \text{----------(6)}$$

Due to reactions (1)–(3), C (mainly graphite) was oxidised leaving the decarburised porous layer in the microstructure. The aggregates from this decarburized layer goes into the metal and or /slag as an inclusion, thus causing the erosion of the refactory.

The variation of erosion resistance for different substitutions of alumina aggregates were as shown in the Figures 5.25-5.27. Figure 5.25 shows the variation of erosion depth when BFA is replaced by WFA aggregates. It has been found that the substitution of BFA by WFA leads to a decrease in erosion depth (increase in erosion resistance). This may be due to the reactivity difference between the BFA and WFA aggregates with the slag used in this investigation. The lower purity level of BFA leads to more chemical reaction with the slag as compared with that of WFA. Thus the erosion depth decreases with increase in WFA substitution to BFA. The variation of erosion depth as a function of BFA substitution to TA is shown in Fig.5.26. It could be observed that the erosion depth increases with increase in BFA substitution. The increase in erosion depth with increase in BFA replacement may be correlated to the chemical reactivity of

BFA and TA. The lower purity level of BFA leads to more chemical reaction with the slag as compared with that of TA. Thus the erosion depth increases with increase in TA substitution by BFA. Figure 5.27 shows the variation of erosion depth as a function of WFA substitution by TA. The nature of graph clearly indicates that the erosion depth decreases when the substitution of WFA is made by TA. In the case the predominant erosion mechanism is the oxidation of C as both the aggregates have almost equivalent chemical nature. The micropore presents in WFA provides the path for oxygen transport to C oxidation. Hence, the erosion depth decreases with TA replacement in WFA.More confirmation about the erosion in the samples has been correlated with respect to XRD analysis of the corroded samples (Fig.5.29). The eroded samples after rotary slag test are shown in the figure 5.28.

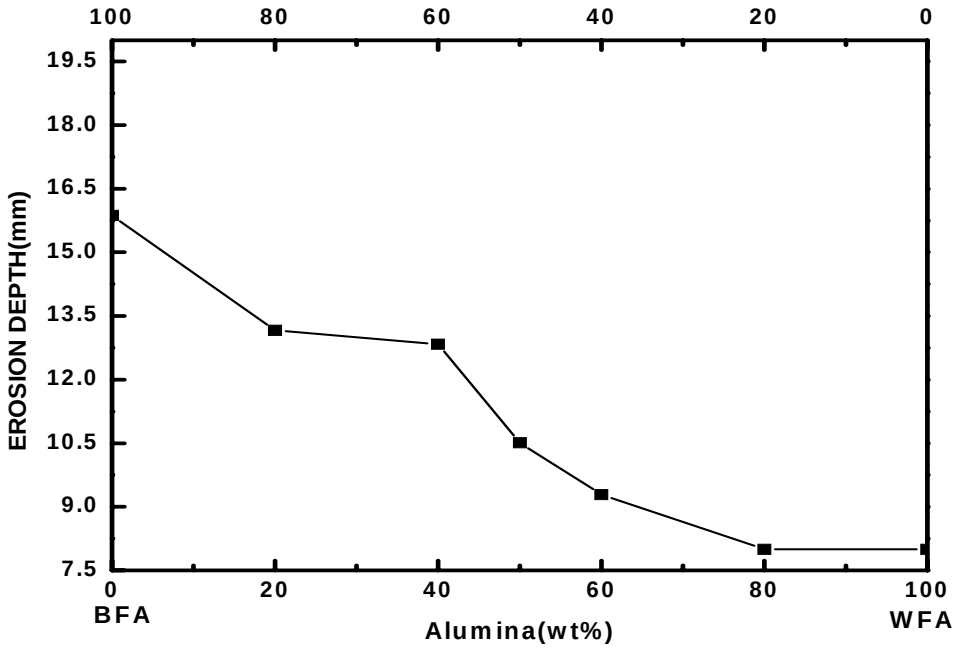

Fig.5.25 Variation of Erosion depth for the sample containing WFA and BFA

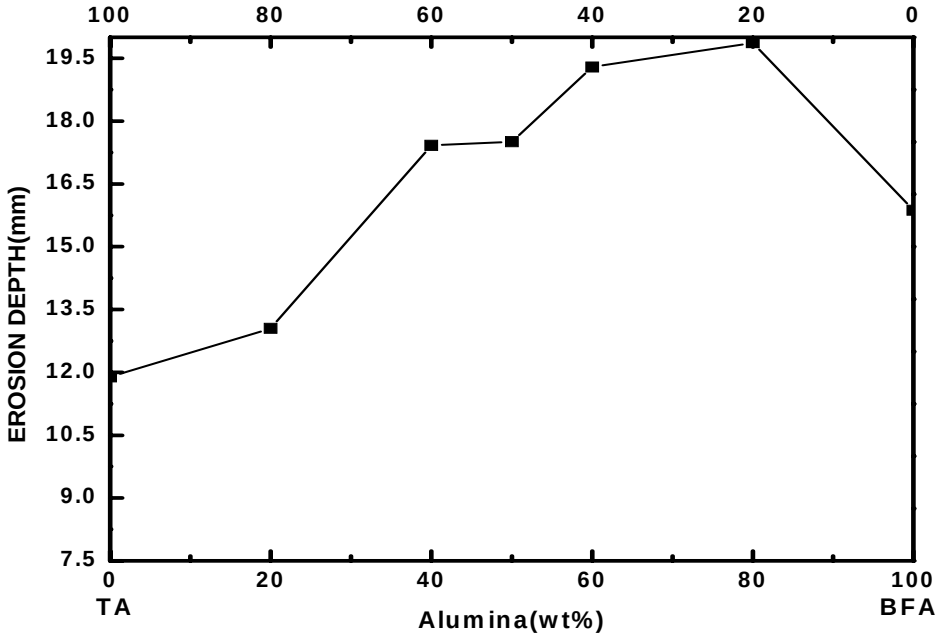

Fig.5.26 Variation of Erosion depth for the sample containing BFA and TA

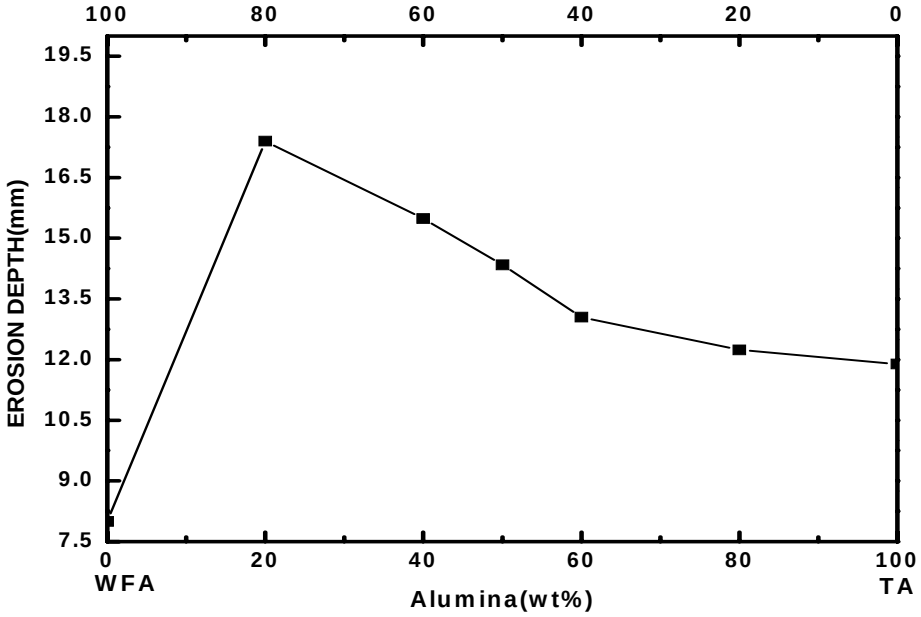

Fig.5.27 Variation of Erosion depth for the sample containing TA and WFA

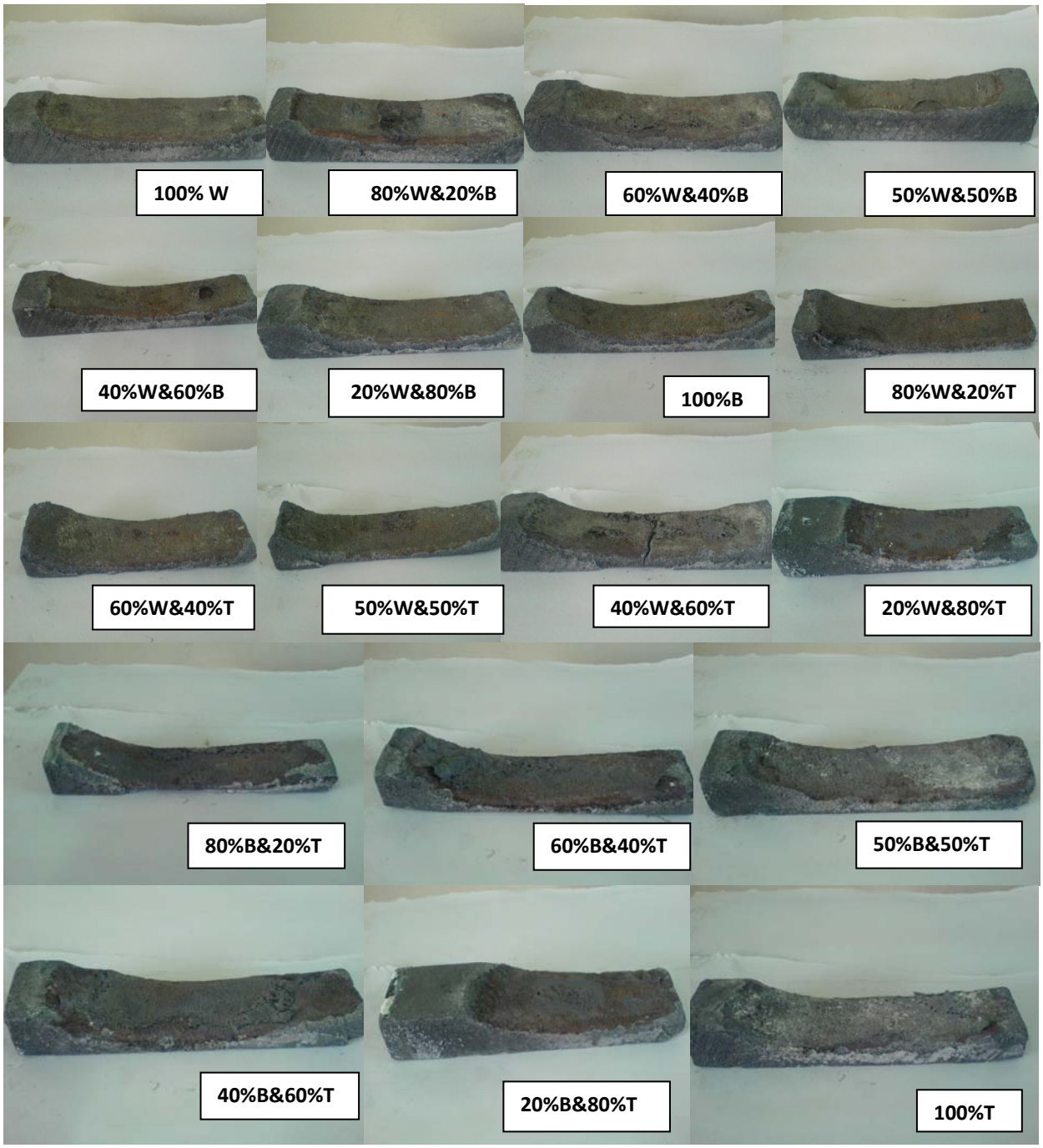

(Fig.5.28 Eroded Alumina –Carbon samples after rotary slag test)

Symbolic representation-W(White fused alumina),B(Brown fused alumina),T(Tabular alumina)

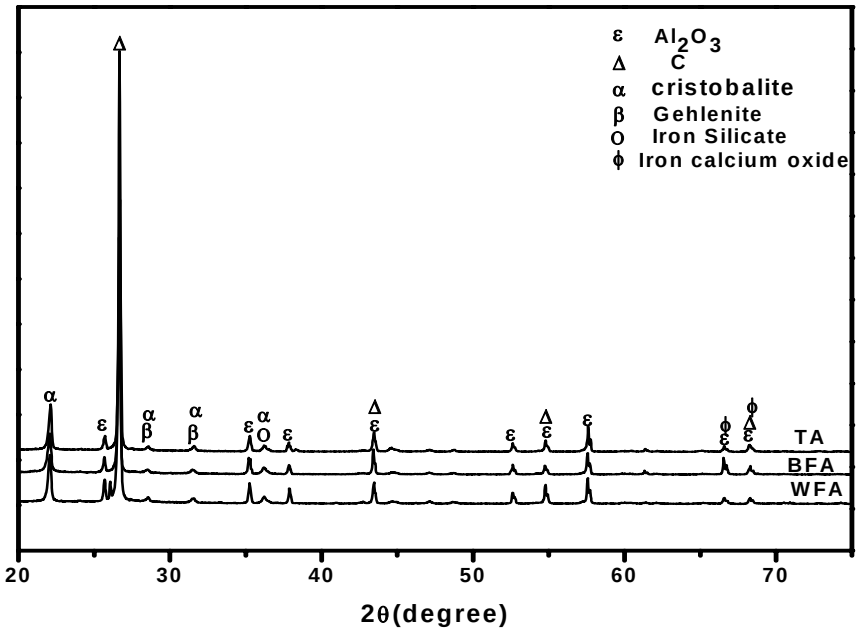

Fig.5.29 XRD pattern of corroded 100% WFA,BFA and TA containing samples

The XRD pattern for corroded samples shows that the formation of low melting phases like gehlenite, iron silicate and iron calcium oxide were responsible for dissolution of refractory into the slag. As the test temperature was above 1500^0C, hence higher amount of CO(g) formation may be responsible for the conversion of SiO_2 into cristobalite. Formation of higher amount of this phase leads to dissolution of refractory into the slag and hence the erosion in the refractory.

5.9 Thermal Spalling Resistance

The thermal spalling test has been done by air quenching method. Different alumina-carbon samples were heat treated at 1200^0C in an oxygen atmosphere for 30 minutes. Prior to the thermal spalling test, the samples were being coated with high temperature coating material. After 30 minutes, the samples were taken out and placed in air for 10 minutes. The process was repeated for 10 cycles and it was found that no crack formation on the surface of sample before 10 cycles of heat treatment followed by air quenching.

5.10 Effect of Antioxidant on the properties of Alumina-Carbon refractories

The effect of metallic silicon powder on the physical,mechanical and thermochemical properties of Alumina-Carbon refractories have been studied and discussed as follows:-

5.10.1 Apparent Porosity and Bulk Density

The variation of metallic silicon addition on AP of the sample containing WFA, BFA and TA aggregates with respect to different wt% silicon is shown in the Fig.5.27. The AP of the samples was found to decrease with the increase in metallic silicon powder addition irrespective of the alumina aggregates.

The decrease in AP value as a function of metallic Si powder addition may be explained as follows. Antioxidants (e.g Si metal powder) play important role by preventing oxidation of carbon bond due to two mechanisms i.e.(i) they themselves melt or form low melting glassy phase and coats the carbon bonds to protect them from being oxidized or (ii) they themselves get oxidized and reduce the partial pressure of oxygen available to oxidize carbon bond. Hence the oxidation of carbon from the sample surface is suppressed with increase in metallic Si addition. This reduction of surface oxygen oxidation with increase in metallic Si addition causes the decrease in AP. The BD of the samples was found to have the reverse trend as compared to AP with metallic Si addition, which is very much obvious. The Fig. 5.30 also shows that the AP of the samples containing WFA aggregates has the highest AP than that of BFA, which has the lowest AP, whereas the samples prepared with TA has an intermediate value irrespective of the metallic Si addition. This could be explained from the particle size distribution (Fig.5.4) and particle morphology of the aggregates. BFA aggregates has more fine fraction which could filled up the inter-aggregate voids and thus provides lower AP in the samples even without metallic additive. The flaky nature of the WFA on the other hand with less fine fraction is attributed for the attainment of higher AP in the samples. Although the TA aggregates has some inherent porosity due their origin attains an intermediate value because of the bimodal distribution of the aggregates.

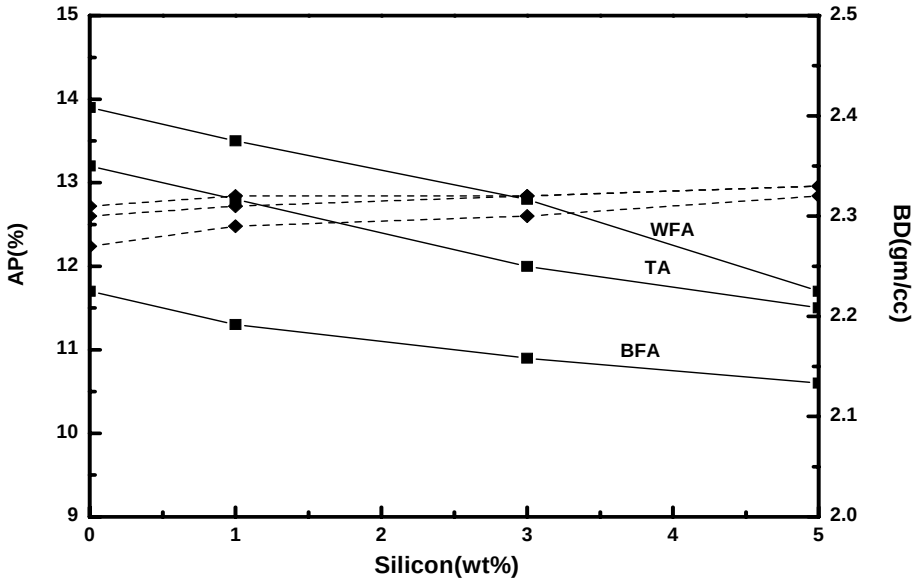

Fig.5.30 Variation of A.P with different silicon (wt%) content for different alumina aggregates

Representation (-------AP) and (——BD)

5.10.2 Cold Modulus of Rupture

The variation of modulus of rupture (MOR) as a function of metallic Si content in the samples containing different alumina aggregates is shown in Fig.5.31 The Fig.5.31 shows that the incorporation of metallic silicon powder into the refractory aggregate leads to increase in MOR irrespective of the aggregates used. The increase in strength due to the metallic Si addition is due to lower oxidation of surface carbon on metal addition. The prominent effect at 5% Si addition is due to the homogeneous mixing of the metal additive. It has also been found that the sample containing TA aggregate show higher MOR value in comparison to WFA, which shows the lower MOR value irrespective of the metal addition. On the other hand samples prepared with BFA have an intermediate MOR value. The attainment of highest MOR value in TA sample is due to the better bonding of the TA aggregates with the resin bond due the inherent rough and porous surface of the aggregates. Samples prepared with WFA aggregates showed the lowest

value as the surface of the WFA aggregates is quite smooth when compared with the other aggregates as well as the high AP of the samples

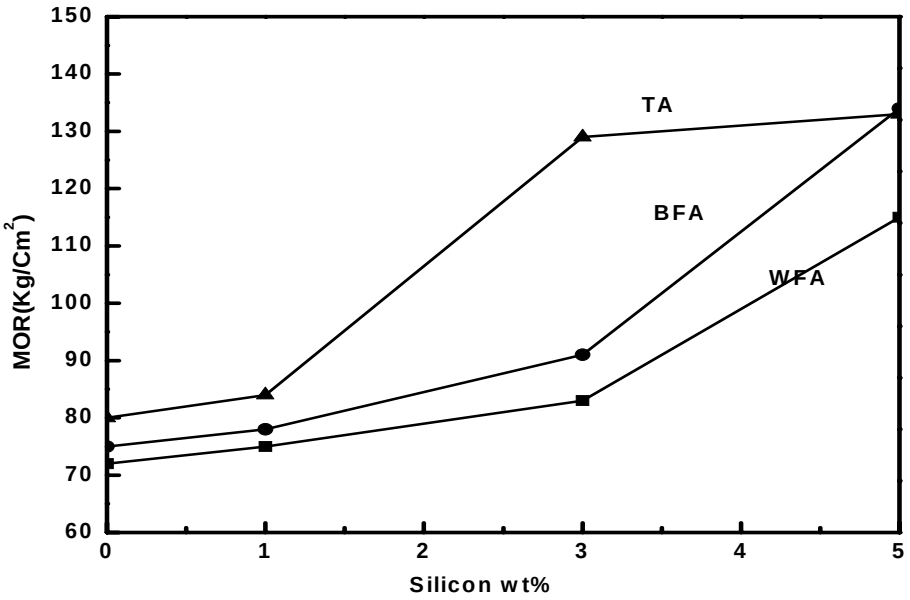

Fig.5.31 Variation of MOR with different silicon(wt%)content for different alumina aggregates

5.10.3 Cold Crushing Strength

The variation of cold crushing strength (CCS) with respect to different alumina aggregates as well as metallic silicon powder addition is shown in Fig.5.32. This figure shows that the CCS increases with increase in metallic silicon addition i.e from 1wt% to 5 wt% irrespective of the alumina aggregates. The addition of higher amount of metallic additive leads to higher crushing strength is due to the lower oxidation of the surface carbon with increase in metallic Si addition. It has also been found that the sample containing TA aggregate show higher CCS value as compared to samples prepared with WFA aggregates which shows the lower value. The samples prepared with BFA have an intermediate value. The same could be explained from the bonding behavior of the aggregates as explained earlier.

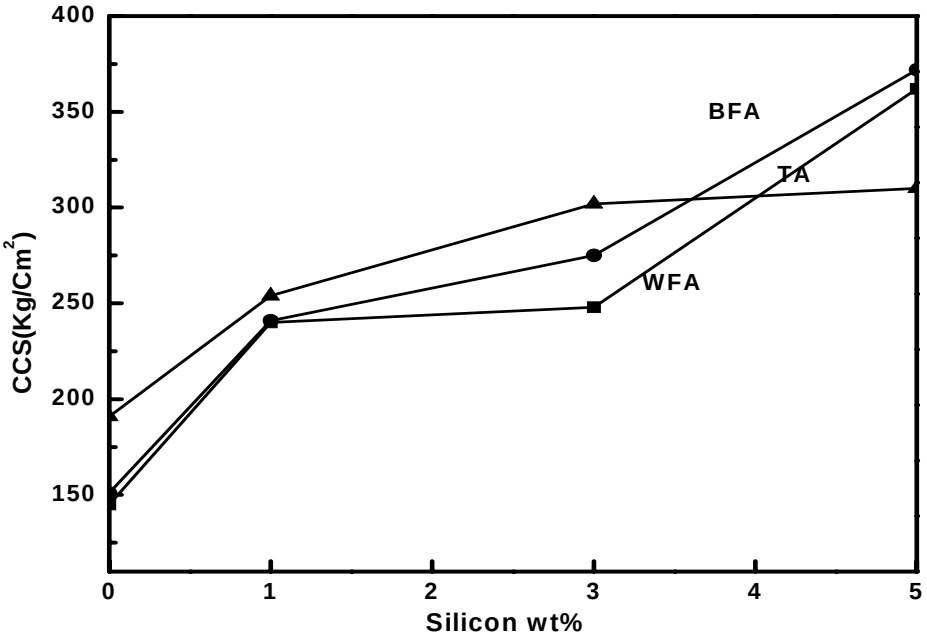

Fig. 5.32 Variation of CCS with different silicon(wt%) content for different alumina aggregates

5.10.4 Oxidation Resistance

Figure 5.33-5.34 shows the variation of oxidation depth with metallic silicon on the samples prepared with different alumina aggregates. The figures clearly indicate that increase in metallic silicon powder addition causes a decrease in oxidation thickness of the refractory sample irrespective of the aggregates used. The more affinity to metallic silicon towards oxygen as compared to carbon inhibits the oxidation of carbon. Thus the samples containing higher amount of metal powder shows better oxidation resistance (lower oxidation layer thickness). Samples prepared with WFA showed the lowest and that prepared with BFA showed the highest oxidation resistance, where as the samples prepared with TA has an intermediate value. This could be explained from the AP of the samples prepared with different alumina aggregates. The samples prepared with WFA have the highest AP and that prepared with BFA aggregates has the lowest AP whereas the sample prepared with TA has an intermediate value (Fig.5.30). This porosity present in the samples provides the path for oxygen diffusion for carbon oxidation. Thus the increased AP in the sample will show low oxidation resistance (more oxidation layer thickness).

The temperature effect on the oxidation resistance could be seen from the figure 5.33-5.34 . It has been found that with increase in temperature the oxidation resistance decreases for the all the samples studied. The decrease in oxidation resistance with increase in test temperature is attributed with the increase in oxygen diffusion and the enhancement of oxidation reaction with increase in temperature.

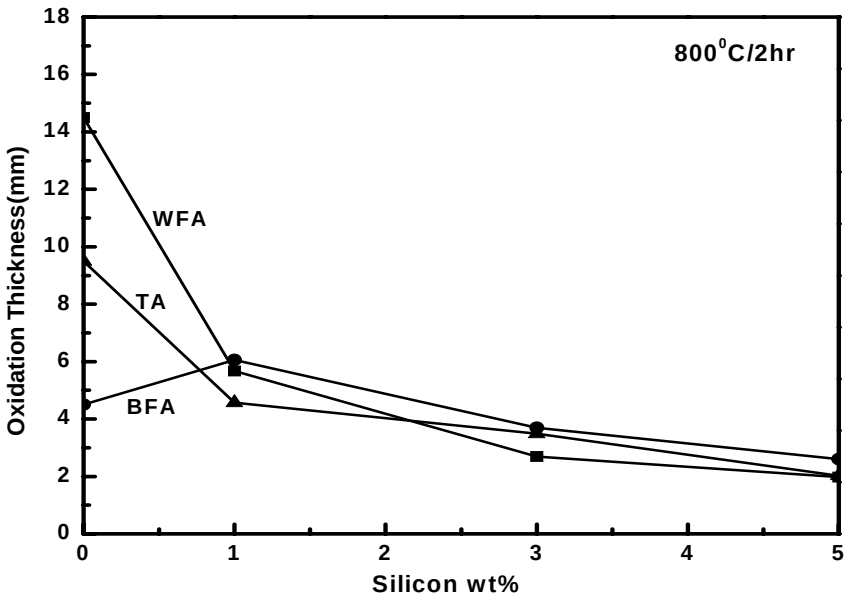

Fig.5.33 Variation of oxidation thickness for different 100% samples heat treated for 2 hr of soaking period

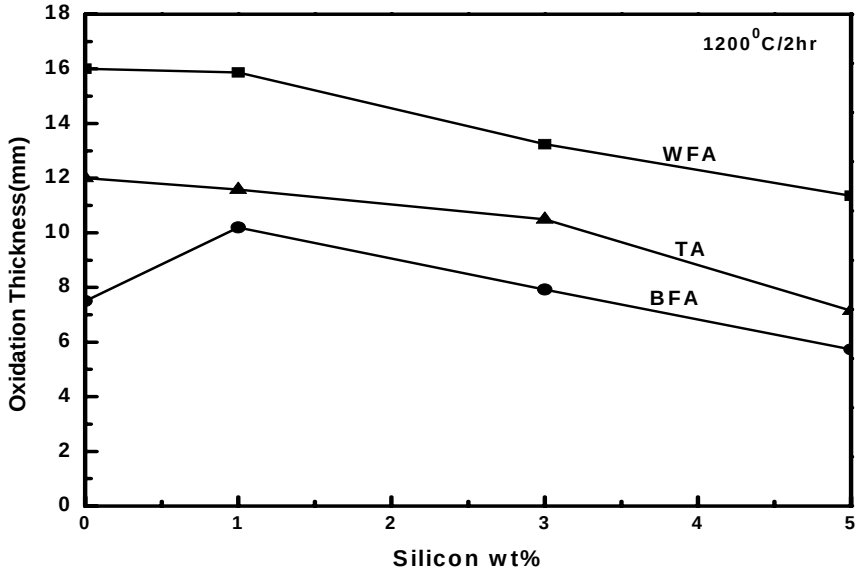

Fig.5.34. Variation of oxidation thickness for different 100% samples heat treated for 2hr of soaking period

5.10.5 Erosion Resistance

The variation of erosion depth with metallic silicon powder addition as well as alumina aggregates used is shown in the Fig.5.35. The erosion depth was found to increase with increase in metallic silicon additive (1-5%) irrespective of the aggregates used.

The effect of Si addition on the Al_2O_3 dissolution may be related to the formation and dissolution of SiO_2 in the slag. The metallic Si used melts at high temperature, coat the carbon surface thus provides a protective layer for inhibition of carbon oxidation. This liquid Si reacts with the graphite and may for SiC as shown in Eqn. (7). At high temperature the Si liquid may reacts with CO and from SiO(g) as by Eqn. (8). The SiC formed by Eqn. (7) may react with CO and formed SiO_2(S) as shown in Eqn. (9). The SiO(g) formed in the uncorroded layer or the penetrated layer would diffuse towards the slag layer, when it arrived at the decarburized layer (the dense Al_2O_3 and/or slag layers), it would be oxidised to SiO_2 via Eqn. (9). The dissolution of SiO_2 in the local slag would decrease the slag basicity (CaO/SiO_2 ratio) and thus increase Al_2O_3 solubility in the

slag and hence greatly accelerate the erosion of the refractory [29]. The reaction mechanism for the formation of SiO_2 is as shown below:-

$$Si(l) + C(s) \longrightarrow SiC(s) \quad \text{----------(7)}$$

$$2Si(l) + 2CO(g) \longrightarrow 2SiO(g) + 2C(s) \quad \text{----------(8)}$$

$$2SiC(s) + 2CO(g) \longrightarrow 2SiO_2(s) + 4C(s) \quad \text{----------(9)}$$

The sample containing BFA aggregates shows higher erosion than the sample containing TA and BFA. This difference can be explained by means of impurity factor in the respective aggregates. As the BFA aggregate has more impure phase than TA and WFA aggregates, hence the erosion will be more in the sample containing BFA.

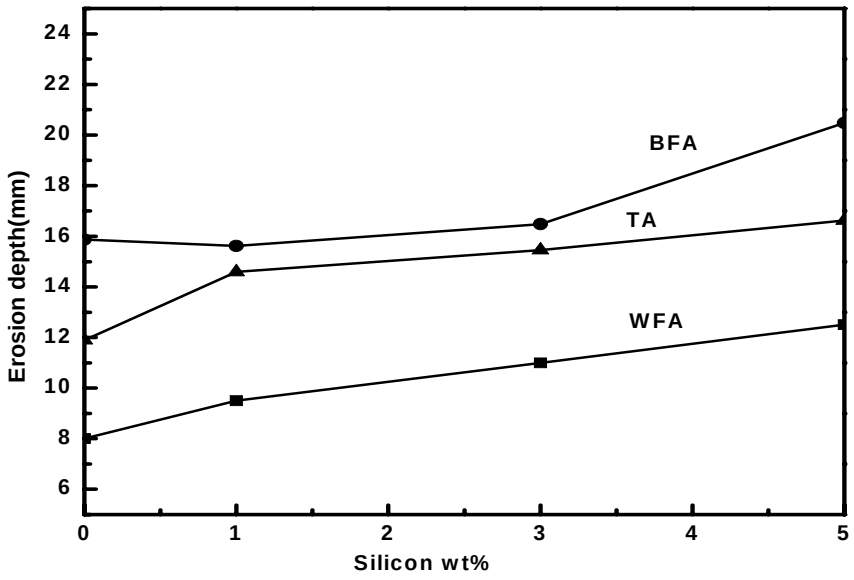

Fig.5.35 Variation of Erosion depth with different silicon(wt%) content for different alumina aggregates

The eroded Al_2O_3-C samples containing silicon additives in different weight proportion were shown as below (Fig.5.36), which shows different erosion depths for WFA, BFA and TA containing aggregates.

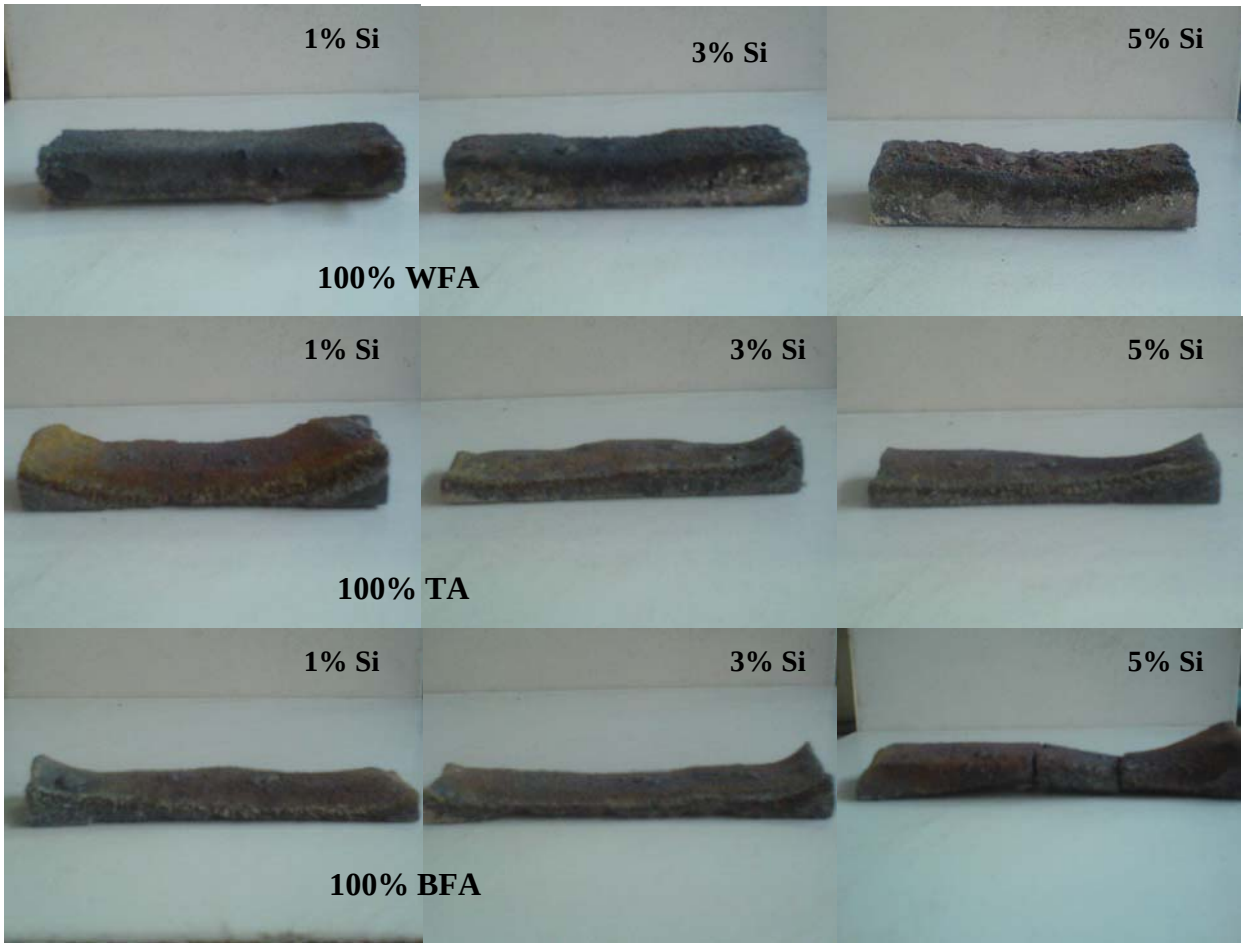

Fig.5.36 The eroded Al_2O_3-C samples containing different weight proportion silicon

CHAPTER 6

Chapter 6 Conclusions & Scope of Future Work

The effect of different alumina aggregates on the properties of Al_2O_3-C refractories has been investigated and discussed. The conclusions of the present study are summarized below:-

(a) Al_2O_3-C refractory samples without antioxidant

1. The AP increases when WFA aggregates have been substituted into BFA aggregate where as the incorporation of BFA to TA was found to decrease AP. The substitution of TA to WFA was found to lower the AP. These variations in AP are in consistence with the particle size, particle size distribution and the morphology of the individual aggregates. Although the variation was negligible, the BD follows a reverse trend as that of AP.

2**.** The mechanical properties (MOR and CCS) of the fired Al_2O_3-C refractories were dependent on the alumina aggregates type and amount used in the brick recipe. The variations were found quite substantial although the variation was negligible in physical properties (AP and BD).

3. The MOE of the fired Al_2O_3-C refractories are dependent on the alumina aggregate morphology.

4. The TEC of the fired Al_2O_3-C refractories are also dependent on the alumina aggregate used in the brick formulation and follows the additive rule.

5. The oxidation of carbon in fired Al_2O_3-C refractories is dependent on the alumina aggregates and increases with increase in test temperature. The oxidation resistance dependence on the alumina aggregates are correlated with the alumina aggregate morphology.

6**.** The erosion resistance of Al_2O_3-C refractories depends on the alumina aggregates used. The dependence was in agreement with chemical nature and aggregate porosity.

(b) Al_2O_3-C refractory samples with metallic silicon antioxidant

1. Metallic silicon powder addition enhances properties like MOR, CCS and oxidation resistance as compared with that without any antioxidant. The improvements were more prominent with increase in metallic silicon addition.

2. The erosion resistance of fired Al_2O_3-C refractories deteriorated with silicon metallic powder addition.

The effect of different alumina aggregates on the performances of alumina-carbon refractories has been studied. An unexplainable result has been found in the MOR and CCS value for 20wt % substitution of one alumina aggregate by another alumina aggregate. However certain important properties like thermal conductivity, thermal shock resistance have not been studied in the thesis work, which were also the requirements for Al_2O_3-C refractories. Hence, the scope of future study may be summarized as below:-

- To study the fluctuation associated with 20 wt% substitution of alumina aggregates
- To measure the thermal conductivity of the alumina-carbon refractories
- To determine the thermal shock parameters for the alumina-carbon refractories
- Detail phase and microstructural study for correlating the observed properties.

References

1. Emad.Mohamed M.Ewais, Carbon based refractories, Journal of the Ceramic Society of Japan,112[10]2004,517-532

2. Chester,J.H.,Refractories production and properties,The iron and steel institute,London,Carlton house,Terrace,pp(10-11)

3. Mukai, K. et al.,A Mechanism for the Local Corrosion of Immersion Nozzles, ISIJ International. Vol. 29 (1989), No. 6, pp. 469 476

4. Buchel,G. *et al.* Review of Tabular Alumina as higher performance Refractory Material, Interceram (2007), pp (6-12

5. Kriechbaum,G.W *et al.*Review on the properties and application of tabular alumina in refractories

6. Advanced seminar on refractories for steel making ,2005, pp(68-69)

7. Kryvoruchko, P. *et al.*, Properties dependence of alumina refractories on the kind of the used alumina – either sintered or fused**,** UNITECR'2007,vol-II,pp(264-267)

8. Javadpour ,J. *et al.*, The effect of additives on the properties and microstructures of Al_2O_3-C refractories, Journal of Material Science 41 (2006) 3027–3032.

9. Guoqi ,Liu. *et al.*, Effect of Composite Metal Additives on Properties of Al_2O_3-Graphite Composites,UNITECR'07,Vol.I,pp(82-86)

10. Zhang, S. *et al.*, Behaviour of antioxidants added to carbon containing refractories, UNITECR'95,Vol.(II),pp(341-348)
11. Bernard B. Argent *et al*., Prediction of the Effect of Additives on Slag resistance of $A1_20_3$-SiO_2-SiC-C Bond Phases in Air, Elsevier Science Ltd, Vol. 27, No. 1, pp. 115-125,(2003)
12. Jingkun, Yu, *et al.*, Synthesis of ZrO_2-SiC composite and effect of its addition on the oxidation resistance of Al_2O_3-C refractory ,Journal of Chinese Academy of Sciences, 72 Wenhua Road, Shenyang, 110015, China,Vol.43(10)2007,pp(1059-1064)

13. Hub´alkov´,J. *et al.,* Microstructure evaluation of MgO–C refractories with TiO_2- and Al-additions, Journal of the European Ceramic Society 27 (2007) 73–78
14. Gurcan, C. *et al.,* The effect of antioxidants on the oxidation behaviour of magnesia–carbon refractory bricks, Ceramics International 34 (2008) 323–330
15. Nemati ,Z. A. *et al.,* The Effect of Ferrosilicon-Silicon Antioxidant on the Properties of Magnesia-Graphite Refractory,UNITECR'03, VOL.I,pp(440-443)
16. Krivokorytov, E. V. *et al*., Effect of antioxidants on the properties of unfired carbon-bearing refractories, Journal of Refractories and Industrial ceramics 40(1999),529-533
17. Hoshiyama, Y. *et al.,* Behavior of Al_4SiC_4 added to the carbon containing refractories, UNITECR'2007,vol-II,pp278-281
18. Kryvoruchko, P .*et al.,* Properties dependence of alumina refractories on the kind of the used alumina – either sintered or fused**,** UNITECR'2007,vol-II,pp(264-267)
19. Sridhar, S. *et al*., The interaction of spherical Al_2O_3 particles with molten Al_2O_3-CaO-FeO_X-SiO_2 slags,Fuel 88(2009) 670-682
20. Junhu, Liu *et al,* In Situ Observation of the Dissolution of Spherical Alumina Particles in CaO–Al_2O_3–SiO_2 Melts, Journal of American Ceramic Society, 90 [12] 3818–3824 (2007)
21. Zhang S, *et al*., Alumina dissolution into silicate slag, Journal of American ceramic society,83[4]897-903(2000)
22. Qingcai, Liu *et al.*, Corrosion resistance of high-alumina graphite based refractories to the smelting reduction melts,UNITECR'05, Vol.(II),pp(105-110)
23. Zhao, L *et al.* ,Interfacial Phenomena during wetting of Graphite/Alumina mixtures by Liquid Iron, ISIJ International, Vol. 43 (2003), No. 1, pp. 1–6
24. Hong, L *et al.,* Investigation of *in-situ* Chemical Reactions of Al_2O_3–SiC–SiO_2–C refractory and Its Interactions with Slag, ISIJ International, Vol. 44 (2004), No. 5, pp. 785–789
25. Khanna, R. *et al.*, Role of Ash Impurities in the Depletion of Carbon from Alumina–Graphite Mixtures in to Liquid Iron, ISIJ International, Vol. 47 (2007), No. 2, pp. 282–288
26. Sasai, K. *et al.,* Reaction Rate between Alumina Graphite Immersion Nozzle and Low Carbon Steel, ISIJ International, Vol. 35 (1995), No. 1, pp. 26-33

27. Sunayama, H. *et al*., Corrosion behavior of MgO-C refractory accompanied by bubble formation in molten slag,UNITECR-2005,Vol-I,pp(6-10)
28. Li Zushu, *et al*., Reactions between Metal, MgO-C Refractory and Molten Slag, ISIJ International, Vol. 40 (2000), Supplement, pp. l01 -105
29. Zhang,S. *et al.,* Influence of additives on corrosion resistance and corroded microstructures of MgO–C refractories, Journal of the European Ceramic Society 21 (2001) 2393–2405
30. Lee W.E *et al.,* Penetration and corrosion of magnesia grain by silicate slags,British Ceramic Transactions,Vol.99,No.6 (June 2000),pp248-255(8)
31. Baldo ,J.B. *et al.,* Key features of alumina/magnesia/graphite refractories for steel Ladle lining, Journal of the European Ceramic Society 20 (2000) 1419-1427
32. Pötschke, J. *et al*., Properties and Corrosion of AMC-Refractories,UNITECR-2003,Vol-II, pp(602-605)
33. Bavand-Vandchali, M. *et al*., Atmosphere and carbon effects on microstructure and phase analysis of in situ spinel formation in MgO-C refractories matrix., Ceramic International 35(2009)861-868
34. Ghosh, N. K.et al. Oxidation mechanism of MgO-C in air at various temperatures, British ceramic transactions , vol. 99(2000) pp. 124-128
35. Guoqi L. *et al.,* The influence of heat-treating atmospheres on Al_2O_3-C materials with Al addition,UNITECR'05, Vol-I,pp(45-49)
36. Nemati, Z.A.,*et al*., Effects of resin and graphite content on density and oxidation behavior of MgO-C refractory bricks, Ceramics International 32 (2006) 313–319
37. Ivashchenko, L. V. et al., Properties and behavior of periclase-carbon systems during the firing-process under oxidizing conditions, Journal of refractories and industrial ceramics 28(1987),301-305
38. Farahani, J. et al., The effect of firing procedure and additives on the microstructure and properties of Al_2O_3-C composites,pp(1-6)
39. Hocquet,S. et al.,Characterisation of oxidation phenomena in carbon containing refractory materials for metallurgy,UNITECR'07,Vol-I,pp(226-229)
40. Budnikov,P.P, The technology of ceramics and refractories,pp(40-43)